Event-Triggered Adaptive Control of a Parabolic PDE–ODE Cascade With Piecewise-Constant Inputs and Identification

Ji Wang, *Member, IEEE*, and Miroslav Krstic, *Fellow, IEEE*

***Abstract*—We present an adaptive event-triggered boundary control scheme for a parabolic partial differential equation–ordinary differential equation (PDE–ODE) system, where the reaction coefficient of the parabolic PDE and the system parameter of a scalar ODE, are unknown. In the proposed controller, the parameter estimates, which are built by batch least-square identification, are recomputed and the plant states are resampled simultaneously. As a result, both the parameter estimates and the control input employ piecewise-constant values. In the closed-loop system, the following results are proved: 1) the absence of a Zeno phenomenon; 2) finite-time exact identification of the unknown parameters under most initial conditions of the plant (all initial conditions except a set of measure zero); and 3) exponential regulation of the plant states to zero. A simulation example is presented to validate the theoretical result.**

***Index Terms*—Adaptive control, backstepping, event-triggered control, least-squares identifier, parabolic PDEs.**

I. Introduction

A. Boundary Control of Parabolic PDEs

Parabolic partial differential equations (PDEs) are predominately used in describing fluid, thermal, and chemical dynamics, including many applications of sea ice melting and freezing [28], [61], continuous casting of steel [41] and lithium-ion batteries [27], [51]. These therefore give rise to related important control and estimation problems of parabolic PDEs.

The backstepping approach has been verified as a very powerful tool for boundary stabilization of PDEs, with many advantages, such as avoiding operator Riccati equations that are very hard to solve for PDEs, and no need for model reduction that often plays an important role in most methods for PDE control design [32, Ch. 1]. The first backstepping boundary control design for parabolic PDEs was introduced in [35] and [36]. Subsequently, more results about boundary control of parabolic PDEs have emerged in the past decade, such as [5], [8], [9], [39], [40], and [42]. In addition to the backstepping method, a forwarding approach, which was first introduced in [38], is also applied to stabilize the hyperbolic PDE systems in [37] and [53], and parabolic PDEs in [6].

In addition to the aforementioned works on parabolic PDEs, topics concerning parabolic PDE–ODE coupled systems are also popular, which have a rich physical background, such as coupled electromagnetic, coupled mechanical, and coupled chemical reactions [50]. Backstepping stabilization of a parabolic PDE in cascade with a linear ODE has been primarily presented in [30] with Dirichlet-type boundary interconnection and, the results on Neuman boundary interconnection were presented in [48] and [50]. Besides, backstepping boundary control designs of a parabolic PDE sandwiched by two ODEs were presented in [10] and [55].

In this article, we deal with a cascade of reaction–diffusion PDE and ODE. For the reaction–diffusion PDE subsystem, the reaction term perturbs the diffusion behavior of the basic heat equation, and there would be many unstable eigenvalues for a positive and large reaction coefficient. Besides, the ODE subsystem also can be in an unstable form when the system parameter is positive.

B. Event-Triggered Control of PDEs

When implementing the continuous-in-time controllers into digital platforms, sampling needs to be addressed properly to ensure the stability of the closed-loop system. Compared with periodical sampling, i.e., sampled-data scheme [21], the event-triggered strategy is more efficient in the aspect of using communication and computational resources, because the sampling happens only when needed.

Most current event-triggered control are designed for ODE systems, such as in [17], [19], [45], and [49]. For event-triggered control in PDE systems, some pioneering attempts were proposed relaying on distributed (in-domain) control inputs [44], [62] or modal decomposition [25], [26]. Recently, using the infinite-dimensional control approach, the state-feedback event-triggered boundary control for a class of 2×2 hyperbolic PDEs was first presented in [14], and then was extended to the output-feedback case in [12]. Output-feedback event-trigged

Manuscript received 17 July 2022; accepted 20 November 2022. Date of publication 9 December 2022; date of current version 30 August 2023. This work was supported in part by the National Natural Science Foundation of China under Grant 62203372 and in part by the Science and Technology Projects of Innovation Laboratory for Sciences and Technologies of Energy Materials of Fujian Province (IKKEM) under Grant HRCP-[2022]-69. Recommended by Associate Editor V. Andrieu. *(Corresponding author: Ji Wang.)*

Ji Wang is with the Department of Automation, Xiamen University, Xiamen, Fujian 361005, China, and also with the Innovation Laboratory for Sciences and Technologies of Energy Materials of Fujian Province (IKKEM), Xiamen, Fujian 361005, China (e-mail: jiwang9024@gmail.com).

Miroslav Krstic is with the Department of Mechanical and Aerospace Engineering, University of California, San Diego, La Jolla, CA 92093-0411 USA (e-mail: krstic@ucsd.edu).

Color versions of one or more figures in this article are available at https://doi.org/10.1109/TAC.2022.3227916.

Digital Object Identifier 10.1109/TAC.2022.3227916

boundary control of a sandwich hyperbolic PDE system was also proposed in [56]. For parabolic PDEs, some important results on event-triggered boundary control were presented in [15], [25], and [43], on the basis of the backstepping method and the modal decomposition approach, respectively. The abovementioned event-triggered control design only focused on a PDE plant with completely known parameters while there always exist some plant parameters not known exactly in practice, which creates a need for incorporating adaptive technology.

C. Triggered Adaptive Control of PDEs

Three traditional adaptive schemes are the Lyapunov design, the passivity-based design, and the swapping design [29], which were initially developed for ODEs in [31], and extended to parabolic PDEs in [1], [2], [33], [34], [46], and [47], and hyperbolic PDEs in [3], [7].

A new adaptive scheme, using a regulation-triggered batch least-square identifier (BaLSI), was introduced in [20] and [22], which has at least two significant advantages over the previous traditional adaptive approaches: guaranteeing exponential regulation of the states to zero, as well as finite-time convergence of the estimates to the true values. An application of this new adaptive scheme to a two-link manipulator, which is modeled by a highly nonlinear ODE system and subject to four parametric uncertainties, was shown in [4]. Regarding PDEs, this method has been applied in adaptive control of a parabolic PDE in [24], and of first-order hyperbolic PDEs in [58] and [60]. In the above designs, the triggering is employed for the parameter estimator (update law), rather than the control law, where the plant states are not sampled. Conversely, in [57], an event-triggered adaptive control design was proposed by employing triggering for the control law instead of the parameter estimator, where only asymptotic convergence is achieved. Recently, a triggered adaptive control design, where the triggering is employed for updating both the parameter estimator and the plant states in the control law, is proposed for hyperbolic PDEs in [59]. This article is the parabolic cousin of [59]. As a result, both the parameter estimates and the control input employ piecewise-constant values, and exponential regulation of the states in the parabolic PDE–ODE cascade is achieved.

D. Contributions

1) As compared to the previous results in [15] and [43] on event-triggered backstepping control for parabolic PDEs with completely known plant parameters, uncertain plant parameters and additional ODE dynamics are considered in this article.
2) Different from adaptive control designs of parabolic PDEs in [33], [46], and [47] where the control input is continuous-in-time, in this article, the control signal is piecewise-constant, and, moreover, the exact parameter identification (for all initial conditions of the plant except a set of measure zero) as well as exponential regulation to zero of the plant states are achieved.
3) Compared with the triggered-type adaptive control designs for parabolic PDE in [24], where triggering is only employed for the parameter update law rather than the plant states in the controller, in this article, triggering is employed for both updating the parameter estimator and resampling the plant states in the controller and, as a result, both the parameter estimates and the control input employ piecewise-constant values. Moreover, an additional uncertain ODE at the uncontrolled boundary of the parabolic PDE is considered in this article.
4) To the best of our knowledge, this is the first adaptive event-triggered boundary control result of parabolic PDEs. The result is new even if the ODE dynamics is removed.

E. Organization

The problem formulation is shown in Section II. The nominal continuous-in-time control design is presented in Section III. The design of event-triggered control with piecewise-constant parameter identification is proposed in Section IV. The absence of a Zeno phenomenon, parameter estimate convergence, and exponential regulation are proved in Section V. The effectiveness of the proposed design is illustrated by a numerical example in Section VI. Finally, Section VII concludes this article.

F. Notation

We adopt the following notation.

1) The symbol $\mathbb{N}$ denotes the set of natural numbers including zero, and the notation $\mathbb{N}^*$ for the set $\{1, 2, \ldots\}$, i.e., the natural numbers without 0. We also denote $\mathbb{R}_+ := [0, +\infty)$ and $\mathbb{R}_- := (-\infty, 0)$.
2) Let $U \subseteq \mathbb{R}^n$ be a set with nonempty interior and let $\Omega \subseteq \mathbb{R}$ be a set. By $C^0(U; \Omega)$, we denote the class of continuous mappings on U, which take values in Ω. By $C^k(U; \Omega)$, where $k \geq 1$, we denote the class of continuous functions on U, which have continuous derivatives of order k on U and take values in Ω.
3) We use the notation $L^2(0, 1)$ for the standard space of the equivalence class of square-integrable, measurable functions defined on $(0, 1)$ and $\|f\| = \left(\int_0^1 f(x)^2 dx\right)^{\frac{1}{2}} < +\infty$ for $f \in L^2(0, 1)$.
4) For an $I \subseteq \mathbb{R}_+$, the space $C^0(I; L^2(0, 1))$ is the space of continuous mappings $I \ni t \mapsto u[t] \in L^2(0, 1)$.
5) Let $u : \mathbb{R}_+ \times [0, 1] \to \mathbb{R}$ be given. We use the notation $u[t]$ to denote the profile of u at certain $t \geq 0$, i.e., $(u[t])(x) = u(x, t)$, for all $x \in [0, 1]$.

II. Problem Formulation

We conduct the control design based on the following parabolic PDE–ODE system:

$$\dot{\zeta}(t) = a\zeta(t) + bu(0, t) \tag{1}$$

$$u_t(x, t) = \varepsilon u_{xx}(x, t) + \lambda u(x, t) \tag{2}$$

$$u_x(0, t) = 0 \tag{3}$$

$$u_x(1, t) + qu(1, t) = U(t) \tag{4}$$

for $x \in [0, 1], t \in [0, \infty)$, where $\zeta(t)$ is a scalar ODE state and $u(x, t)$ is a PDE state. The function $U(t)$ is the control input to be designed. The parameters $\varepsilon, \lambda,$ and a are arbitrary, and $b \neq 0$. The ODE system parameter a and the coefficient λ of the PDE in-domain couplings are unknown.

Assumption 1: The bounds of the unknown parameters λ and a are known and arbitrary, i.e., $\underline{\lambda} \leq \lambda \leq \overline{\lambda}$, $\underline{a} \leq a \leq \overline{a}$, where $\underline{\lambda}, \overline{\lambda}, \overline{a},$ and $\underline{a}$ are arbitrary positive constants whose values are known.

We define a vector θ that includes the two unknown parameters λ and a, i.e.,

$$\theta = [\lambda, a]^T. \tag{5}$$

Assumption 2: The parameter q satisfies

$$q > \frac{1}{4} + \frac{\overline{\lambda}}{2\varepsilon}.$$

Assumption 2 avoids the use of the signal $u(1,t)$ in the nominal control law, whose purpose is to ensure no Zeno behavior in the event-based system. For the reaction–diffusion equation, an eigenfunction expansion of the solution of (2)–(4) with $U(t) = 0$ shows that the parabolic PDE system is unstable when $\lambda > \varepsilon\pi^2/4$, no matter what $q > 0$ is [43].

The motivation of the considered PDE–ODE cascade is from control of uncertain thermal-fluid systems [54] with uncertain finite-dimensional sensor dynamics. We only consider a scalar ODE in this article with the purpose of presenting the proposed control design more clearly. With a modest modification, the result in this article is possible to extend to the case that the ODE state is a vector and the system matrix and input matrix in the ODE are linear functions of unknown parameters. We reiterate here that the result in this article is new even if the ODE (1) is absent.

III. Nominal Control Design

In the nominal control design, similar to [10], we apply three transformations to convert the original plant (1)–(4) to an exponentially stable target system.

We introduce the following backstepping transformation [32, (4.55)]:

$$w(x,t) = u(x,t) - \int_0^x \Psi(x,y)u(y,t)dy \tag{6}$$

where

$$\Psi(x,y) = -\frac{\lambda}{\varepsilon}x\frac{I_1(\sqrt{\lambda(x^2-y^2)/\varepsilon})}{\sqrt{\lambda(x^2-y^2)/\varepsilon}} \tag{7}$$

and I_1 denotes the modified Bessel functions of the first kind, to convert the plant (1)–(4) to the system

$$\dot{\zeta}(t) = a\zeta(t) + bw(0,t) \tag{8}$$

$$w_t(x,t) = \varepsilon w_{xx}(x,t) \tag{9}$$

$$w_x(0,t) = 0 \tag{10}$$

$$\begin{aligned} w_x(1,t) + rw(1,t) = {} & U(t) + (r - q - \Psi(1,1))u(1,t) \\ & - \int_0^1 \Big(\Psi_x(1,y) + q\Psi(1,y) \\ & + \Psi(1,y)(r-q)\Big)u(y,t)dy \end{aligned} \tag{11}$$

where r is a positive constant that will be determined later.

Following [32, Sec. 4.5], the inverse transformation of (6) is shown as

$$u(x,t) = w(x,t) + \int_0^x \Phi(x,y)w(y,t)dy \tag{12}$$

where

$$\Phi(x,y) = -\frac{\lambda}{\varepsilon}x\frac{J_1(\sqrt{\lambda(x^2-y^2)/\varepsilon})}{\sqrt{\lambda(x^2-y^2)/\varepsilon}} \tag{13}$$

and J_1 denotes the (nonmodified) Bessel functions of the first kind.

Applying the second transformation,

$$v(x,t) = w(x,t) - \gamma(x)\zeta(t) \tag{14}$$

where

$$\gamma(x) = -\kappa\cos\left(\sqrt{\frac{(b\kappa - a)}{\varepsilon}}x\right) \tag{15}$$

we convert the system (8)–(11) into the following intermediate system:

$$\dot{\zeta}(t) = -a_{\mathrm{m}}\zeta(t) + bv(0,t) \tag{16}$$

$$v_t(x,t) = \varepsilon v_{xx}(x,t) - \gamma(x)bv(0,t) \tag{17}$$

$$v_x(0,t) = 0 \tag{18}$$

$$\begin{aligned} v_x(1,t) + rv(1,t) = {} & U(t) - \gamma'(1)\zeta(t) - r\gamma(1)\zeta(t) \\ & + (r - q - \Psi(1,1))u(1,t) \\ & - \int_0^1 \Big(\Psi_x(1,y) + q\Psi(1,y) \\ & + \Psi(1,y)(r-q)\Big)u(y,t)dy \end{aligned} \tag{19}$$

where

$$a_{\mathrm{m}} = b\kappa - a > 0 \tag{20}$$

is ensured by a design parameter κ satisfying

$$\kappa > \frac{\overline{a}}{b}. \tag{21}$$

See Appendix A for the calculation of the conditions of $\gamma(x)$ by matching (8)–(11) and (16)–(19) via (14).

We introduce the third transformation

$$\beta(x,t) = v(x,t) - \int_0^x h(x,y)v(y,t)dy \tag{22}$$

where the kernel $h(x,y)$ is to be determined, to convert (16)–(19) into the target system

$$\dot{\zeta}(t) = -a_{\mathrm{m}}\zeta(t) + b\beta(0,t) \tag{23}$$

$$\beta_t(x,t) = \varepsilon\beta_{xx}(x,t) \tag{24}$$

$$\beta_x(0,t) = 0 \tag{25}$$

$$\beta_x(1,t) = -r\beta(1,t) \tag{26}$$

where

$$r = q + \Psi(1,1) + h(1,1) = q - \frac{\lambda}{2\varepsilon} > \frac{1}{4} \tag{27}$$

with recalling $\Psi(1,1) = -\frac{\lambda}{2\varepsilon}$ considering (7), and $h(1,1) = 0$ is derived from the last two conditions of $h(x,y)$, which are shown next, and Assumption 2.

By matching (23)–(25) and (16)–(18) via (22) (see Appendix B for details), the conditions of $h(x,y)$ are obtained as

$$h_y(x,0)\varepsilon + \gamma(x)b - b\int_0^x h(x,y)\gamma(y)dy = 0 \tag{28}$$

$$h_{yy}(x,y) - h_{xx}(x,y) = 0 \tag{29}$$

$$h_y(x,x) + h_x(x,x) = 0 \tag{30}$$

$$h(0,0) = 0 \tag{31}$$

which is covered by the ones found in [11] which ensures that (28)–(31) have a piecewise C_2-solution.

For (26) to hold, the control input is chosen as

$$U(t) = \int_0^1 K_1(1,y;\theta)u(y,t)dy + K_2(1;\theta)\zeta(t) \tag{32}$$

where

$$\begin{aligned} K_1(1,y;\theta) &= \Psi_x(1,y) + h_x(1,y) + rh(1,y) \\ &\quad + \left(q - \frac{\lambda}{2\varepsilon}\right)\Psi(1,y) \\ &\quad - \int_y^1 (h_x(1,z) + rh(1,z))\Psi(z,y)dz \end{aligned} \tag{33}$$

$$\begin{aligned} K_2(1;\theta) &= \gamma'(1) + \left(q - \frac{\lambda}{2\varepsilon}\right)\gamma(1) \\ &\quad - \int_0^1 (h_x(1,y) + rh(1,y))\gamma(y)dy. \end{aligned} \tag{34}$$

Writing $\theta = [\lambda, a]^T$ in K_1 and K_2 emphasizes the fact that K_1 and K_2 depend on the unknown parameters λ and a (the kernels $\Psi, \gamma,$ and h defined in (7), (15), and (28)–(31) include these unknown parameters).

According to [10], there exists kernel $h^I(x,y) \in \mathbb{R}$ for the inverse transformation of (22), which is shown as

$$v(x,t) = \beta(x,t) - \int_0^x h^I(x,y)\beta(y,t)dy. \tag{35}$$

In summary, with the purpose of building the nominal control law, in this section, we apply three transformations to convert the original system to the target system. The first transformation is to "eliminate" the reaction term $\lambda u(x,t)$, which is a source of instability, in (2). Then, we are to make the ODE (1) in a stable form with compensating heat PDE dynamics at its input, like [30]. We use the second transformation (14) to make the system coefficient of the ODE (1) as negative, and apply the last transformation to compensate the residual term $\gamma(x)bv(0,t)$, which results from applying the second transformation, in (17).

IV. Event-Triggered Control Design With Piecewise-Constant Parameter Identification

Based on the nominal continuous-in-time feedback (32), we give the form of an adaptive event-triggered control law U_d, as follows:

$$\begin{aligned} U_{di} := U_d(t_i) = &\int_0^1 K_1(1,y;\hat{\theta}(t_i))u(y,t_i)dy \\ &+ K_2(1;\hat{\theta}(t_i))\zeta(t_i) \end{aligned} \tag{36}$$

for $t \in [t_i, t_{i+1})$, where

$$\hat{\theta} = [\hat{\lambda}, \hat{a}]^T \tag{37}$$

is an estimate, which is generated with a triggered BaLSI, of the two unknown parameters λ and a. The identifier and the sequence of time instants $\{t_i \geq 0\}_{i=0}^{\infty}$, $i \in \mathbb{N}$, are defined in the next section.

Inserting the piecewise-constant control input U_{di} into (4), the boundary condition becomes

$$u_x(1,t) + qu(1,t) = U_{di}. \tag{38}$$

When we mention the continuous-in-state control signal U_c, we refer to the signal consisting of triggered parameter estimates and continuous states, i.e.,

$$U_c(t) = \int_0^1 K_1(1,y;\hat{\theta}(t_i))u(y,t)dy + K_2(1;\hat{\theta}(t_i))\zeta(t) \tag{39}$$

for $t \in [t_i, t_{i+1})$. The signal U_c does not act as the control input of the plant but used in the event-triggering mechanism (ETM), which will be shown latter.

Define the difference between the continuous-in-state control signal U_c in (39) and the event-triggered control input U_d in (36) as $d(t)$, given by

$$\begin{aligned} d(t) &= U_c(t) - U_{di} \\ &= \int_0^1 K_1(1,y;\hat{\theta}(t_i))(u(y,t) - u(y,t_i))dy \\ &\quad + K_2(1;\hat{\theta}(t_i))(\zeta(t) - \zeta(t_i)) \end{aligned} \tag{40}$$

for $t \in [t_i, t_{i+1})$, which reflects the deviation of the plant states from their sampled values and will be used in building the ETM.

Define the difference between the continuous-in-state control signal $U_c(t)$ in (39) and the nominal continuous-in-time control input $U(t)$ in (32) as $p(t)$, given by

$$\begin{aligned} p(t) &= U(t) - U_c(t) \\ &= \int_0^1 (K_1(1,y;\theta) - K_1(1,y;\hat{\theta}(t_i)))u(y,t)dy \\ &\quad + (K_2(1;\theta) - K_2(1;\hat{\theta}(t_i)))\zeta(t),\ t \in [t_i, t_{i+1}) \end{aligned} \tag{41}$$

which reflects the deviation of the estimates from the actual unknown parameters.

The deviations $d(t)$ and $p(t)$ will be used in the following design and analysis.

A. ETM

The sequence of time instants $\{t_i \geq 0\}_{i=0}^{\infty}$ $(t_0 = 0)$ is defined as

$$t_{i+1} = \min\{\inf\{t > t_i : d(t)^2 \geq -\xi m(t)\}, t_i + T\} \tag{42}$$

where the positive constant ξ is a design parameter, and another design parameter $T > 0$ sets the maximum dwell-time with the purpose of avoiding the less frequent updates of the parameter estimates, which may lead to a large overshoot in the response of the closed-loop system.

The dynamic variable $m(t)$ in (42) satisfies the ordinary differential equation

$$\dot{m}(t) = -\eta m(t) + \lambda_d d(t)^2 - \kappa_1 u(1,t)^2 - \kappa_2 u(0,t)^2 - \kappa_3 \|u(\cdot,t)\|^2 - \kappa_4 \zeta(t)^2 \tag{43}$$

for $t \in (t_i, t_{i+1})$ with $m(t_0) = m(0) < 0$, and $m(t_i^-) = m(t_i) = m(t_i^+)$. Here, t_i^+ and t_i^- are the right and left limits of $t = t_i$. It is worth noting that the initial condition for $m(t)$ in each time interval has been chosen such that $m(t)$ is time continuous. The positive design parameters $\kappa_1, \kappa_2, \kappa_3,$ and κ_4 are determined later. Inserting $d(t)^2 \le -\xi m(t)$ guaranteed by (42) into (43), we have

$$\dot{m}(t) \le -(\eta + \lambda_d \xi) m(t) - \kappa_1 u(1,t)^2 - \kappa_2 u(0,t)^2 - \kappa_3 \|u(\cdot,t)\|^2 - \kappa_4 \zeta(t)^2. \tag{44}$$

Next, we show $m(t) < 0$ all the time under $m(0) < 0$. Multiplying both sides of (44) by $e^{(\eta+\lambda_d\xi)t}$, then moving $e^{(\eta+\lambda_d\xi)t}(\eta + \lambda_d \xi) m(t)$ from the right-hand side to the left-hand side, yields

$$\begin{aligned} &\dot{m}(t)e^{(\eta+\lambda_d\xi)t} + e^{(\eta+\lambda_d\xi)t}(\eta+\lambda_d\xi)m(t) \\ &\le -e^{(\eta+\lambda_d\xi)t}(\kappa_1 u(1,t)^2 + \kappa_2 u(0,t)^2 \\ &\quad + \kappa_3\|u(\cdot,t)\|^2 + \kappa_4\zeta(t)^2). \end{aligned}$$

That is,

$$\frac{d(m(t)e^{(\eta+\lambda_d\xi)t})}{dt} \le -e^{(\eta+\lambda_d\xi)t}\left(\kappa_1 u(1,t)^2 + \kappa_2 u(0,t)^2 + \kappa_3\|u(\cdot,t)\|^2 + \kappa_4\zeta(t)^2\right). \tag{45}$$

Integration of (45) from 0 to t yields

$$\begin{aligned} m(t) \le\ & m(0)e^{-(\eta+\lambda_d\xi)t} \\ & - \int_0^t e^{-(\eta+\lambda_d\xi)(t-\varrho)}\left(\kappa_1 u(1,\varrho)^2 + \kappa_2 u(0,\varrho)^2 \right. \\ & \left. + \kappa_3\|u(\cdot,\varrho)\|^2 + \kappa_4\zeta(\varrho)^2\right) d\varrho. \end{aligned} \tag{46}$$

Because $m(0) < 0$, both terms on the right-hand side of (46) are less than zero. Therefore, $m(t) < 0$.

For the proposed ETM (42), the maximal dwell-time is T. For some design parameters $\kappa_1, \kappa_2, \kappa_3,$ and κ_4, the minimal dwell-time is larger than a positive constant, i.e., no Zeno behavior, which will be proved in Lemma 2.

B. BaLSI

According to (1) and (2), we get for $\tau > 0$ and $n \in \mathbb{N}^*$ that

$$\begin{aligned} &\frac{d}{d\tau}\left(\int_0^1 \sin(x\pi n)u(x,\tau)dx - \frac{1}{b}\varepsilon\pi n\zeta(\tau)\right) \\ &= \varepsilon\int_0^1 \sin(x\pi n)u_{xx}(x,\tau)dx \\ &\quad + \lambda\int_0^1 \sin(x\pi n)u(x,\tau)dx - \frac{1}{b}\varepsilon\pi n\dot{\zeta}(\tau) \\ &= -\varepsilon\pi n\cos(\pi n)u(1,\tau) + \varepsilon\pi n u(0,\tau) \\ &\quad - \frac{a}{b}\varepsilon\pi n\zeta(\tau) - \varepsilon\pi n u(0,\tau) \\ &\quad - \varepsilon\pi^2 n^2\int_0^1 \sin(x\pi n)u(x,\tau)dx + \lambda\int_0^1 \sin(x\pi n)u(x,\tau)dx \\ &= -\varepsilon\pi n\cos(\pi n)u(1,\tau) - \varepsilon\pi^2 n^2\int_0^1 \sin(x\pi n)u(x,\tau)dx \\ &\quad + \lambda\int_0^1 \sin(x\pi n)u(x,\tau)dx - \frac{1}{b}a\varepsilon\pi n\zeta(\tau). \end{aligned} \tag{47}$$

Define

$$\mu_{i+1} := \min\{t_d : d \in \{0,\dots,i\}, t_d \ge t_{i+1} - \tilde{N}T\} \tag{48}$$

according to [22], where the positive integer $\tilde{N} \ge 1$ is a free design parameter (a larger $\tilde{N}$ will make the least-squares identifier run based on a bigger set of data, which makes the identifier more robust with respect to measurement errors), and the positive constant T is the maximum dwell-time in (42). Integrating (47) from μ_{i+1} to t yields

$$f_n(t,\mu_{i+1}) = \lambda g_{n,1}(t,\mu_{i+1}) + a g_{n,2}(t,\mu_{i+1}) \tag{49}$$

where

$$\begin{aligned} f_n(t,\mu_{i+1}) =\ & \int_0^1 \sin(x\pi n)u(x,t)dx - \frac{1}{b}\varepsilon\pi n\zeta(t) \\ & - \int_0^1 \sin(x\pi n)u(x,\mu_{i+1})dx + \frac{1}{b}\varepsilon\pi n\zeta(\mu_{i+1}) \\ & + \int_{\mu_{i+1}}^t \Big[\varepsilon\pi n(-1)^n u(1,\tau) \\ & + \varepsilon\pi^2 n^2\int_0^1 \sin(x\pi n)u(x,\tau)dx\Big] d\tau \end{aligned} \tag{50}$$

$$g_{n,1}(t,\mu_{i+1}) = \int_{\mu_{i+1}}^t \int_0^1 \sin(x\pi n)u(x,\tau)dxd\tau \tag{51}$$

$$g_{n,2}(t,\mu_{i+1}) = -\frac{1}{b}\varepsilon\pi n\int_{\mu_{i+1}}^t \zeta(\tau)d\tau \tag{52}$$

for $n \in \mathbb{N}^*$.

Define the function $h_{i,n} : \mathbb{R}^2 \to \mathbb{R}_+$ by the formula:

$$h_{i,n}(\ell) = \int_{\mu_{i+1}}^{t_{i+1}} \left(f_n(t,\mu_{i+1}) - \ell_1 g_{n,1}(t,\mu_{i+1}) - \ell_2 g_{n,2}(t,\mu_{i+1})\right)^2 dt \tag{53}$$

for $i \in \mathbb{N}$, $n \in \mathbb{N}^*$, and $\ell = [\ell_1, \ell_2]^T$.

According to (49), the function $h_{i,n}(\ell)$ in (53) has a global minimum $h_{i,n}(\theta) = 0$. According to [24], applying Fermat's theorem (of extrema)—that is, differentiating the functions $h_{i,n}(\ell)$ defined by (53) with respect to ℓ_1, ℓ_2, respectively, and making the derivatives at the position of the global minimum $(\ell_1, \ell_2) = (\lambda, a)$ as zero—we have that the following matrix equation hold for every $i \in \mathbb{N}$ and $n \in \mathbb{N}^*$:

$$Z_n(\mu_{i+1}, t_{i+1}) = G_n(\mu_{i+1}, t_{i+1})\theta \tag{54}$$

where

$$Z_n(\mu_{i+1}, t_{i+1}) = [H_{n,1}(\mu_{i+1}, t_{i+1}), H_{n,2}(\mu_{i+1}, t_{i+1})]^T \tag{55}$$

$$G_n(\mu_{i+1}, t_{i+1}) = \begin{bmatrix} Q_{n,1}(\mu_{i+1}, t_{i+1}) & Q_{n,2}(\mu_{i+1}, t_{i+1}) \\ Q_{n,2}(\mu_{i+1}, t_{i+1}) & Q_{n,3}(\mu_{i+1}, t_{i+1}) \end{bmatrix} \tag{56}$$

with

$$H_{n,1}(\mu_{i+1}, t_{i+1}) = \int_{\mu_{i+1}}^{t_{i+1}} g_{n,1}(t, \mu_{i+1}) f_n(t, \mu_{i+1}) dt \tag{57}$$

$$H_{n,2}(\mu_{i+1}, t_{i+1}) = \int_{\mu_{i+1}}^{t_{i+1}} g_{n,2}(t, \mu_{i+1}) f_n(t, \mu_{i+1}) dt \tag{58}$$

$$Q_{n,1}(\mu_{i+1}, t_{i+1}) = \int_{\mu_{i+1}}^{t_{i+1}} g_{n,1}(t, \mu_{i+1})^2 dt \tag{59}$$

$$Q_{n,2}(\mu_{i+1}, t_{i+1}) = \int_{\mu_{i+1}}^{t_{i+1}} g_{n,1}(t, \mu_{i+1}) g_{n,2}(t, \mu_{i+1}) dt \tag{60}$$

$$Q_{n,3}(\mu_{i+1}, t_{i+1}) = \int_{\mu_{i+1}}^{t_{i+1}} g_{n,2}(t, \mu_{i+1})^2 dt. \tag{61}$$

The parameter estimator (update law) is defined as

$$\hat\theta(t_{i+1}) = \text{argmin}\Big\{ |\ell - \hat\theta(t_i)|^2 : \ell \in \Theta, \; Z_n(\mu_{i+1}, t_{i+1}) = G_n(\mu_{i+1}, t_{i+1})\ell, \; n \in \mathbb{N}^* \Big\} \tag{62}$$

where $\Theta = \{\ell \in \mathbb{R}^2 : \underline{\lambda} \le \ell_1 \le \overline{\lambda}, \underline{a} \le \ell_2 \le \overline{a}\}$.

C. Well-Posedness Issues

With the variation-of-constants formula, we write the solution to (1) as

$$\zeta(t) = e^{at}\zeta(0) + b\int_0^t e^{a(t-\tau)} u(0,\tau) d\tau. \tag{63}$$

The well-posedness property is stated as follows.

Proposition 1: Between the time instants t_i and t_{i+1}, for every $u[t_i] \in L^2(0,1)$, $\zeta(t_i) \in \mathbb{R}$, and $m(t_i) \in \mathbb{R}_-$, there exist unique mappings $u \in C^0([t_i, t_{i+1}]; L^2(0,1)) \cap C^1((t_i, t_{i+1}) \times [0,1])$ with $u[t] \in C^2([0,1])$, $\zeta \in C^0([t_i, t_{i+1}]; \mathbb{R})$, and $m \in C^0([t_i, t_{i+1}]; \mathbb{R}_-)$, which satisfy (2), (3), (38), (63), and (43).

Proof: The PDE subsystem (2), (3), (38) is identical to [43, (1a), (1b), (20)]. According to [43, Proposition 4], whose proof depends on [23, Th. 4.11], we have that for every $u[t_i] \in L^2(0,1)$, there exist a unique solution $u \in C^0([t_i, t_{i+1}]; L^2(0,1)) \cap C^1((t_i, t_{i+1}) \times [0,1])$ with $u[t] \in C^2([0,1])$ to (2), (3), and (38). It implies that the signal $\int_0^t u(0,\tau)d\tau$ is time continuous. Considering (63), we obtain $\zeta \in C^0([t_i, t_{i+1}]; \mathbb{R})$. Recalling (46) and the obtained well posedness of the u-PDE and ζ-ODE, we have $m \in C^0([t_i, t_{i+1}]; \mathbb{R}_-)$. Proposition 1 is obtained. ■

Proposition 1 shows the solution of the closed-loop system is unique and defined on $t \in [0, \lim_{i\to\infty}(t_i))$. We will then prove no Zeno behavior in the closed-loop system, which guarantees the solution is defined on $\mathbb{R}_+$.

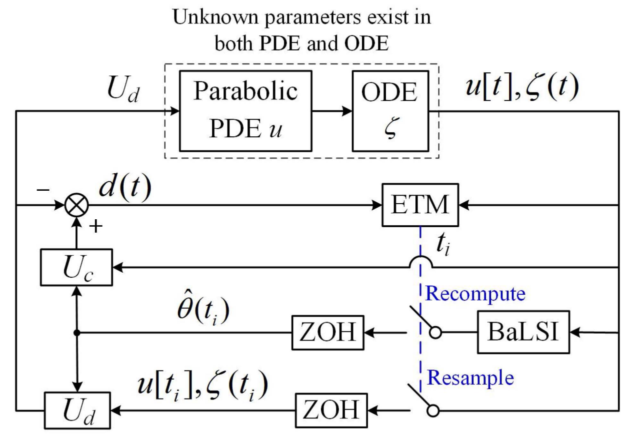

Fig. 1. Block diagram of the closed-loop system.

D. Main Result

The block diagram of the closed-loop system is presented in Fig. 1. The main result of this article is shown as follows.

Theorem 1: For all initial data $u[0] \in L^2(0,1)$, $\zeta(0) \in \mathbb{R}$, $m(0) \in \mathbb{R}_-$, and $\hat\theta(0) \in \Theta_1$, the closed-loop system, i.e., (1)–(4) under the controller (36), with the ETM (42), (43), and the least-squares identifier defined by (62), has the following properties:

1) No Zeno behavior.
2) Except for the case that both $u[0]$ and $\zeta(0)$ are zero, there exist positive constants M, σ (independent of initial data $u[0], \zeta(0)$) such that
$$\Omega(t) \le M\Omega(0)e^{-\sigma t}, \; t \in [0, \infty) \tag{64}$$
where $\Omega(t) = \|u[t]\|^2 + \zeta(t)^2 + |m(t)| + |\tilde\theta(t)|$. The single bars $|\cdot|$ for $\tilde\theta(t) = \theta - \hat\theta(t)$ denotes the Euclidean norm.
3) If both $u[0]$ and $\zeta(0)$ are zero, then $u[t] \equiv 0$, $\zeta(t) \equiv 0$, $m(t) = m(0)e^{-\eta t}$, and $\hat\theta(t) \equiv \hat\theta(0)$ for $t \in [0, \infty)$—that is, all signals are bounded in the sense of
$$\Omega(t) \le |m(0)| + \left|\theta - \hat\theta(0)\right|, \; t \in [0, \infty). \tag{65}$$

Proof: The proof is shown in next section. ■

In the proposed control system, all conditions of the design parameters are cascaded rather than coupled, and only depend on the known parameters. An order of selecting the design parameters is shown in Fig. 2.

Theorem 1 implies the exponential convergence to zero of the plant states $u[t], \zeta(t)$ for all initial data $u[0], \zeta(0)$. The whole states in the closed-loop system include the plant states $u[t], \zeta(t)$, the parameter estimate state $\hat\theta(t)$, and the ETM internal dynamic variable $m(t)$. The exponential convergence of the whole states is achieved, when the initial values of the parameter estimate and ETM internal dynamic variable—that is, $\hat\theta(0), m(0)$ that are chosen by users—are in the given regions.

We take $t_0 = 0$ is just to reduce the notational overload. In all designs and proofs in this article, $t_0 = 0$ makes no difference, i.e., the initial time $t_0 = 0$ can be replaced with a generic t_0.

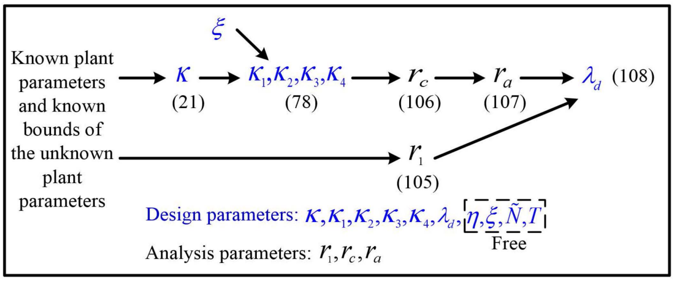

Fig. 2. Order of selecting the design parameters.

V. Proof of Theorem 1

The proof of Theorem 1 is divided into three parts: 1) there is no Zeno behavior, which guarantees the solution of the closed-loop system is unique and is defined on $\mathbb{R}_+$; 2) finite-time exact parameter identification is achieved under most initial conditions; 3) exponential regulation to zero of the plant states is guaranteed. The first part is the proof of the first portion of Theorem 1. The second part (convergence of the parameter estimates) contributes to the third part—that is, the proofs of the last two portions of Theorem 1.

A. No Zeno Behavior

First, we present the following lemma about the upper bound of $\dot{d}(t)^2$, which will be used to show no Zeno behavior.

Lemma 1: For $d(t)$ defined in (40), there exist positive constants $\epsilon_1, \epsilon_2, \epsilon_3, \epsilon_4,$ and ϵ_5 such that

$$\dot{d}(t)^2 \le \epsilon_1 d(t)^2 + \epsilon_2 u(1,t)^2 + \epsilon_3 u(0,t)^2 + \epsilon_4 \|u(\cdot,t)\|^2 + \epsilon_5 \zeta(t)^2 \tag{66}$$

for $t \in (t_i, t_{i+1})$, where $\epsilon_1, \epsilon_2, \epsilon_3, \epsilon_4,$ and ϵ_5 only depend on the design parameter κ in (21), the known plant parameters, and the known bounds $\overline{a}, \underline{a}, \overline{\lambda},$ and $\underline{\lambda}$ of the unknown parameters.

Proof: The event-triggered control input U_d is constant on $t \in (t_i, t_{i+1})$, i.e., $\dot{U}_d(t) = 0$. Recalling Proposition 1, taking the time derivative of (40), recalling (1)–(3), applying integration by parts, we obtain that

$$\begin{aligned} \dot{d}(t) &= \dot{U}_c(t) \\ &= K_1(1,1;\hat{\theta}(t_i))\varepsilon u_x(1,t) - K_{1y}(1,1;\hat{\theta}(t_i))\varepsilon u(1,t) \\ &\quad + K_{1y}(1,0;\hat{\theta}(t_i))\varepsilon u(0,t) \\ &\quad + \int_0^1 K_{1yy}(1,y;\hat{\theta}(t_i))\varepsilon u(y,t)dy \\ &\quad + \int_0^1 K_1(1,y;\hat{\theta}(t_i))\lambda u(y,t)dy \\ &\quad + K_2(1;\hat{\theta}(t_i))a\zeta(t) + K_2(1;\hat{\theta}(t_i))bu(0,t) \end{aligned} \tag{67}$$

for $t \in (t_i, t_{i+1})$. Applying (40) and (41), it allows us to rewrite (38) as

$$u_x(1,t) + qu(1,t) = U(t) - p(t) - d(t). \tag{68}$$

Inserting (68) into (67) to replace $u_x(1,t)$, we then have

$$\begin{aligned} \dot{d}(t) = &- K_1(1,1;\hat{\theta}(t_i))\varepsilon d(t) - K_1(1,1;\hat{\theta}(t_i))\varepsilon p(t) \\ &- (qK_1(1,1;\hat{\theta}(t_i))\varepsilon + K_{1y}(1,1;\hat{\theta}(t_i))\varepsilon)u(1,t) \\ &+ (K_{1y}(1,0;\hat{\theta}(t_i))\varepsilon + K_2(1;\hat{\theta}(t_i))b)u(0,t) \\ &+ \int_0^1 [K_{1yy}(1,y;\hat{\theta}(t_i))\varepsilon + K_1(1,y;\hat{\theta}(t_i))\lambda \\ &+ K_1(1,1;\hat{\theta}(t_i))\varepsilon K_1(1,y;\theta)]u(y,t)dy \\ &+ (K_2(1;\hat{\theta}(t_i))a + K_1(1,1;\hat{\theta}(t_i))\varepsilon K_2(1;\theta))\zeta(t) \end{aligned} \tag{69}$$

for $t \in (t_i, t_{i+1})$, where (32) has been used.

Applying the Cauchy–Schwarz inequality into (41), we have

$$\begin{aligned} p(t)^2 \le\ & 2 \max_{\vartheta_1,\vartheta_2\in\Theta} \left\{ \int_0^1 (K_1(1,y;\vartheta_1) - K_1(1,y;\vartheta_2))^2 dy \right\} \\ & \times \|u[t]\|^2 \\ & + 2 \max_{\vartheta_1,\vartheta_2\in\Theta} \{(K_2(1;\vartheta_1) - K_2(1;\vartheta_2))^2\}\zeta(t)^2. \end{aligned} \tag{70}$$

Applying the Cauchy–Schwarz inequality into (69), using (70), we then obtain (66), where

$$\epsilon_1 = 6\varepsilon^2 \max_{\vartheta\in\Theta}\{K_1(1,1;\vartheta)^2\} \tag{71}$$

$$\epsilon_2 = 6 \max_{\vartheta\in\Theta}\{(qK_1(1,1;\vartheta)\varepsilon + K_{1y}(1,1;\vartheta)\varepsilon)^2\} \tag{72}$$

$$\epsilon_3 = 6 \max_{\vartheta\in\Theta}\{(K_{1y}(1,0;\vartheta)\varepsilon + K_2(1;\vartheta)b)^2\} \tag{73}$$

$$\begin{aligned} \epsilon_4 = & 12 \max_{\vartheta\in\Theta} \left\{ \int_0^1 (K_{1yy}(1,y;\vartheta)\varepsilon + K_1(1,y;\vartheta)\lambda)^2 dy \right\} \\ & + 12\varepsilon^2 \max_{\vartheta\in\Theta}\{K_1(1,1;\vartheta)^2\} \max_{\vartheta\in\Theta} \left\{ \int_0^1 K_1(1,y;\vartheta)^2 dy \right\} \\ & + 12\varepsilon^2 \max_{\vartheta\in\Theta}\{K_1(1,1;\vartheta)^2\} \\ & \times \max_{\vartheta_1,\vartheta_2\in\Theta} \left\{ \int_0^1 (K_1(1,y;\vartheta_1) - K_1(1,y;\vartheta_2))^2 dy \right\} \end{aligned} \tag{74}$$

$$\begin{aligned} \epsilon_5 = & 12\bar{a}^2 \max_{\vartheta\in\Theta}\{(K_2(1;\vartheta)^2\} \\ & + 12\varepsilon^2 \max_{\vartheta\in\Theta}\{K_1(1,1;\vartheta)^2\} \max_{\vartheta\in\Theta} \{K_2(1;\vartheta)^2\} \\ & + 12\varepsilon^2 \max_{\vartheta\in\Theta}\{K_1(1,1;\vartheta)^2\} \\ & \times \max_{\vartheta_1,\vartheta_2\in\Theta}\{(K_2(1;\vartheta_1) - K_2(1;\vartheta_2))^2\}. \end{aligned} \tag{75}$$

The proof of Lemma 1 is complete. ■

Relying on Lemma 1, we then present the following lemma that shows no Zeno behavior.

Lemma 2: For some positive $\kappa_1, \kappa_2, \kappa_3,$ and κ_4, there exists a minimal dwell-time $\underline{\tau} > 0$ such that $t_{i+1} - t_i \ge \underline{\tau}$ for all $i \in \mathbb{N}$.

Proof: 1) If the event is triggered by the second condition, i.e., $t_{i+1} = t_i + T$, in (42), it is obvious that the dwell-time is $T > 0$.

2) Next, we consider the case that the event is triggered by the first condition in (42). Define the following function $\psi(t)$:

$$\psi(t) = \frac{d(t)^2 + \frac{1}{2}\xi m(t)}{-\frac{1}{2}\xi m(t)} \tag{76}$$

which was originally introduced in [14]. We have that $\psi(t_{i+1}) = 1$ because the event is triggered, and that $\psi(t_i) < 0$ because of $d(t_i) = 0$ according to (40). The function $\psi(t)$ is a continuous function on $[t_i^+, t_{i+1}^-]$ recalling (40) and $u \in C^0([t_i, t_{i+1}]; L^2(0,1))$, $\zeta \in C^0([t_i, t_{i+1}]; \mathbb{R})$, $m \in C^0([t_i, t_{i+1}]; \mathbb{R}_-)$ in Proposition 1. By the intermediate value theorem, there exists a $t^* \in (t_i, t_{i+1})$ such that $\psi(t) \in [0,1]$ when $t \in [t^*, t_{i+1}^-]$. The lower bound of dwell-time can be founded as the minimal time it takes for $\psi(t)$ from 0 to 1.

Taking the derivative of (76) for all $t \in [t^*, t_{i+1})$, applying Young's inequality, using (66) in Lemma 1, and inserting (43), we have

$$\begin{aligned}
\dot{\psi} &= \frac{2d(t)\dot{d}(t) + \frac{1}{2}\xi \dot{m}(t)}{-\frac{1}{2}\xi m(t)} - \frac{\dot{m}(t)}{m(t)}\psi \\
&\leq \frac{1}{-\frac{1}{2}\xi m(t)}\Bigg[\epsilon_1 d(t)^2 + \epsilon_2 u(1,t)^2 + \epsilon_3 u(0,t)^2 \\
&\quad + \epsilon_4 \|u(\cdot,t)\|^2 + \epsilon_5 \zeta(t)^2 + d(t)^2 - \frac{1}{2}\xi\eta m(t) \\
&\quad + \frac{1}{2}\xi\lambda_d d(t)^2 - \frac{1}{2}\xi\kappa_1 u(1,t)^2 - \frac{1}{2}\xi\kappa_2 u(0,t)^2 \\
&\quad - \frac{1}{2}\xi\kappa_3 \|u(\cdot,t)\|^2 - \frac{1}{2}\xi\kappa_4 \zeta(t)^2\Bigg] - \frac{\lambda_d d(t)^2}{m(t)}\psi + \eta\psi \\
&\quad - \frac{-\kappa_1 u(1,t)^2 - \kappa_2 u(0,t)^2 - \kappa_3\|u(\cdot,t)\|^2 - \kappa_4\zeta(t)^2}{m(t)}\psi.
\end{aligned} \tag{77}$$

It is worth pointing out that the last term in (77) is less than zero. Choose

$$\kappa_1 \geq \frac{2\epsilon_2}{\xi},\ \kappa_2 \geq \frac{2\epsilon_3}{\xi},\ \kappa_3 \geq \frac{2\epsilon_4}{\xi},\ \kappa_4 \geq \frac{2\epsilon_5}{\xi} \tag{78}$$

where $\epsilon_2, \epsilon_3, \epsilon_4$, and ϵ_5 are given in (72)–(75), which only depend on the design parameter κ in (21), the known plant parameters, and the known bounds $\overline{a}, \underline{a}, \overline{\lambda}$, and $\underline{\lambda}$ of the unknown parameters.

Then, (77) becomes

$$\begin{aligned}
\dot{\psi} &\leq \frac{1}{-\frac{1}{2}\xi m(t)}\left[\left(\epsilon_1 + 1 + \frac{1}{2}\xi\lambda_d\right)d(t)^2 - \frac{1}{2}\xi\eta m(t)\right] \\
&\quad - \frac{\lambda_d d(t)^2}{m(t)}\psi + \eta\psi.
\end{aligned} \tag{79}$$

Inserting

$$\frac{d(t)^2}{m(t)} = \frac{d(t)^2 + \frac{1}{2}\xi m(t) - \frac{1}{2}\xi m(t)}{m(t)} = -\frac{1}{2}\xi\left(\psi(t) + 1\right)$$

we obtain from (79) that

$$\dot{\psi} \leq n_1\psi^2 + n_2\psi + n_3 \tag{80}$$

where $n_1 = \frac{1}{2}\lambda_d\xi$, $n_2 = 1 + \epsilon_1 + \xi\lambda_d + \eta$, and $n_3 = 1 + \eta + \epsilon_1 + \frac{1}{2}\xi\lambda_d$ are positive constants. It follows that the lower bound of dwell-time in this case is

$$\underline{\tau}_a = \int_0^1 \frac{1}{n_3 + n_2 s + n_1 s^2} ds > 0. \tag{81}$$

Together with the result in 1), we have that the minimal dwell-time $\underline{\tau}$ is

$$\underline{\tau} = \min\{\underline{\tau}_a, T\} > 0. \tag{82}$$

The proof of this Lemma is complete. ■

It follows from Lemma 2 that no Zeno phenomenon occurs, i.e., $\lim_{i\to\infty} t_i = +\infty$, which allows the solution of the closed-loop system to be defined on $\mathbb{R}_+$, and guarantee the well-posedness of the closed-loop system recalling Proposition 1.

Corollary 1: For all initial data $u[0] \in L^2(0,1)$, $\zeta(0) \in \mathbb{R}$, and $m(0) \in \mathbb{R}_-$, there exist unique mappings $u \in C^0(\mathbb{R}_+; L^2(0,1)) \bigcap C^1(J \times [0,1])$ with $u[t] \in C^2([0,1])$, $\zeta \in C^0(\mathbb{R}_+; \mathbb{R})$, and $m \in C^0(\mathbb{R}_+; \mathbb{R}_-)$, which satisfy (2), (3), (38), (63), and (46) for $t > 0$, where $J = \mathbb{R}_+ \backslash \{t_i \geq 0, i \in \mathbb{N}\}$.

Proof: For every $u[0] \in L^2(0,1)$, $\zeta(0) \in \mathbb{R}$, $m(0) \in \mathbb{R}_-$, recalling Proposition 1, we have $u \in C^0([0,t_1]; L^2(0,1)) \bigcap C^1((0,t_1) \times [0,1])$ with $u[t] \in C^2([0,1])$, $\zeta \in C^0([0,t_1]; \mathbb{R})$, $m \in C^0([0,t_1]; \mathbb{R}_-)$. It implies that $u[t_1] \in L^2(0,1)$, $\zeta(t_1) \in \mathbb{R}$, $m(t_1) \in \mathbb{R}_-$. Applying Proposition 1 for the interval $[t_1, t_2]$ again, we have the same regularity of the solution. Through a step-by-step construction, applying Proposition 1 repeatedly, we have that $u \in C^0([0, \lim_{i\to\infty} t_i); L^2(0,1)) \bigcap C^1(\bar{J} \times [0,1])$ with $u[t] \in C^2([0,1])$, $\zeta \in C^0([0, \lim_{i\to\infty} t_i); \mathbb{R})$, and $m \in C^0([0, \lim_{i\to\infty} t_i); \mathbb{R}_-)$, where $\bar{J} = [0, \lim_{i\to\infty} t_i) \backslash \{t_i \geq 0, i \in \mathbb{N}\}$. Recalling Lemma 2 that means $\lim_{i\to\infty} t_i = +\infty$, Corollary 1 is obtained. ■

The proof of the first portion in Theorem 1 is complete. In the next section, we will show the convergence of parameter estimates, which will be used in the Lyapunov analysis about exponential regulation of the plant states in the last section, i.e., the proofs of the last two portions in Theorem 1.

B. Convergence of Parameter Estimates

At the beginning of this section, we present the following four lemmas that are required in showing the convergence of parameter estimates.

Lemma 3: For $Q_{n,1}(\mu_{i+1}, t_{i+1})$ and $Q_{n,3}(\mu_{i+1}, t_{i+1})$ defined by (59), (61) and (51), (52), the sufficient and necessary conditions of $Q_{n,1}(\mu_{i+1}, t_{i+1}) = 0$, $Q_{n,3}(\mu_{i+1}, t_{i+1}) = 0$ for all $n \in \mathbb{N}^*$, are $u[t] = 0$, $\zeta(t) = 0$ on $t \in [\mu_{i+1}, t_{i+1}]$, respectively.

Proof: Necessity: If $Q_{n,1}(\mu_{i+1}, \tau_{i+1}) = 0$ for all $n \in \mathbb{N}^*$, then the definition (59) in conjunction with continuity of $g_{n,1}(t, \mu_{i+1})$ for $t \in [\mu_{i+1}, \tau_{i+1}]$ (a consequence of definition (51) and the fact that $u \in C^0([\mu_{i+1}, \tau_{i+1}]; L^2(0,1))$) implies

$$g_{n,1}(t, \mu_{i+1}) = 0,\ t \in [\mu_{i+1}, \tau_{i+1}] \tag{83}$$

for all $n \in \mathbb{N}^*$. According to the definition (51) and continuity of the mapping $\tau \to \int_0^1 \sin(x\pi n) u[\tau] dx$ (a consequence of the fact that $u \in C^0([\mu_{i+1}, \tau_{i+1}]; L^2(0,1))$, (83) implies $\int_0^1 \sin(x\pi n) u(x,\tau) dx = 0$, $\tau \in [\mu_{i+1}, \tau_{i+1}]$ for all $n \in \mathbb{N}^*$. Since the set $\{\sqrt{2}\sin(n\pi x) : n = 1, 2, \ldots\}$ is an orthonormal basis of $L^2(0,1)$, we have $u[t] = 0$ for $t \in [\mu_{i+1}, \tau_{i+1}]$.

Sufficiency: If $u[t]=0$ on $t\in[\mu_{i+1},\tau_{i+1}]$, then $Q_{n,1}(\mu_{i+1},\tau_{i+1})=0$ for all $n\in\mathbb{N}^*$ is obtained directly, according to (51) and (59).

By recalling (52) and (61), the fact that the sufficient and necessary condition of $Q_{3n}(\mu_{i+1},t_{i+1})=0$ for all $n\in\mathbb{N}^*$ is $\zeta(t)=0$ on $t\in[\mu_{i+1},t_{i+1}]$, is obtained straightforwardly.

The proof of Lemma 3 is complete. ■

Lemma 4: For the adaptive estimates defined by (62) based on the data in the interval $t\in[\mu_{i+1},t_{i+1}]$, the following statements hold.

1) If $u[t]$ (or $\zeta(t)$) is not identically zero for $t\in[\mu_{i+1},t_{i+1}]$, then $\hat\lambda(t_{i+1})=\lambda$ (or $\hat a(t_{i+1})=a$).
2) If $u[t]$ (or $\zeta(t)$) is identically zero for $t\in[\mu_{i+1},t_{i+1}]$, then $\hat\lambda(t_{i+1})=\hat\lambda(t_i)$ (or $\hat a(t_{i+1})=\hat a(t_i)$).

Proof: First, we define a set as follows,

$$S_i:=\Big\{\bar\ell=(\ell_1,\ell_2)^T\in\Theta: Z_n(\mu_{i+1},t_{i+1})=G_n(\mu_{i+1},t_{i+1})\bar\ell,\\ n\in\mathbb{N}^*\Big\},\ i\in\mathbb{N} \tag{84}$$

where $\Theta=\{\bar\ell\in\mathbb{R}^2:\underline{\lambda}\le\ell_1\le\overline{\lambda},\underline{a}\le\ell_2\le\overline{a}\}$, and Z_n and G_n in (55) and (56) are associated with the plant states over a time interval $[\mu_{i+1},t_{i+1}]$.

We prove the following four claims, from which the statements in this lemma are concluded.

Claim 1: If $u[t]$ is not identically zero and $\zeta(t)$ is identically zero on $t\in[\mu_{i+1},t_{i+1}]$, then $\hat\lambda(t_{i+1})=\lambda$ and $\hat a(t_{i+1})=\hat a(t_i)$.

Proof: Because $u[t]$ is not identically zero and $\zeta(t)$ is identically zero on $t\in[\mu_{i+1},\tau_{i+1}]$, there exists $n\in\mathbb{N}^*$ such that $Q_{n,1}(\mu_{i+1},\tau_{i+1})\neq0$ recalling Lemma 3. Define the index set I to be the set of all $n\in\mathbb{N}^*$ with $Q_{n,1}(\mu_{i+1},\tau_{i+1})\neq0$. According to (52) and $\zeta(t)$ being identically zero on $t\in[\mu_{i+1},\tau_{i+1}]$, we know that $g_{n,2}(t,\mu_{i+1})=0$ on $t\in[\mu_{i+1},\tau_{i+1}]$ for all $n\in\mathbb{N}^*$. It follows that $Q_{n,2}(\mu_{i+1},\tau_{i+1})=0$, $Q_{n,3}(\mu_{i+1},\tau_{i+1})=0$, and $H_{n,2}(\mu_{i+1},\tau_{i+1})=0$ for all $n\in\mathbb{N}^*$ recalling (60), (61), and (58). Recalling (55) and (56), then (84) implies $S_i=\{(\ell_1,\ell_2)\in\Theta:\ell_1=\frac{H_{n,1}(\mu_{i+1},\tau_{i+1})}{Q_{n,1}(\mu_{i+1},\tau_{i+1})},n\in I\}$. Because $(q_1,q_2)\in S_i$ according to (54), it follows that $S_i=\{(q_1,\ell_2)\in\Theta:\underline{a}\le\ell_2\le\overline{a}\}$. Therefore, (62) shows that $\hat\lambda(\tau_{i+1})=\lambda$ and $\hat a(\tau_{i+1})=\hat a(\tau_i)$. ■

Claim 2: If $u[t]$ is identically zero and $\zeta(t)$ is not identically zero on $t\in[\mu_{i+1},t_{i+1}]$, then $\hat\lambda(t_{i+1})=\hat\lambda(t_i)$ and $\hat a(t_{i+1})=a$.

Proof: The proof of this claim is very similar to the proof of Claim 1, and thus, it is omitted.

Claim 3: If $u[t],\zeta(t)$ are identically zero on $t\in[\mu_{i+1},t_{i+1}]$, then $\hat\lambda(t_{i+1})=\hat\lambda(t_i)$ and $\hat a(t_{i+1})=\hat a(t_i)$.

Proof: In this case, $Q_{n,1}(\mu_{i+1},t_{i+1})=0$, $Q_{n,2}(\mu_{i+1},t_{i+1})=0$, $Q_{n,3}(\mu_{i+1},t_{i+1})=0$, $H_{n,1}(\mu_{i+1},t_{i+1})=0$, and $H_{n,2}(\mu_{i+1},t_{i+1})=0$ for all $n\in\mathbb{N}^*$ according to (51), (52), (57)–(61). It follows that $S_i=\Theta$, and then (62) shows that $\hat\lambda(t_{i+1})=\hat\lambda(t_i)$, $\hat a(t_{i+1})=\hat a(t_i)$. ■

Claim 4: If both $u[t]$ and $\zeta(t)$ are not identically zero on $t\in[\mu_{i+1},t_{i+1}]$, then $\hat\lambda(t_{i+1})=\lambda$ and $\hat a(t_{i+1})=a$.

Proof: By virtue of (54) and (62), if S_i is a singleton, then it is nothing else but the least-squares estimate of the unknown vector of parameters (λ,a) on the interval $[\mu_{i+1},t_{i+1}]$, and $S_i=\{(\lambda,a)\}$. From (55), (56), (84), and Lemma 3, we have that

$$S_i\subseteq S_{ai}:=\Big\{(\ell_1,\ell_2)\in\Theta:\ell_2=\frac{H_{n,2}(\mu_{i+1},t_{i+1})}{Q_{n,3}(\mu_{i+1},t_{i+1})}\\ -\ell_1\frac{Q_{n,2}(\mu_{i+1},t_{i+1})}{Q_{n,3}(\mu_{i+1},t_{i+1})},n\in\mathbb{N}^*\Big\}. \tag{85}$$

We next prove by contradiction that $S_i=\{(\lambda,a)\}$. Suppose that on the contrary $S_i\neq\{(\lambda,a)\}$, i.e., S_i defined by (84) is not a singleton, which implies the set S_{ai} defined by (85) are not singletons (because S_{ai} being a singleton implies that S_i is a singleton). It follows that there exist constants $\bar r\in\mathbb{R}$ such that

$$\frac{Q_{n,2}(\mu_{i+1},t_{i+1})}{Q_{n,3}(\mu_{i+1},t_{i+1})}=\bar r,\ n\in\mathbb{N}^* \tag{86}$$

because if there were two different indices $k_1,k_2\in\mathbb{N}^*$ with $\frac{Q_{k_1,2}(\mu_{i+1},t_{i+1})}{Q_{k_1,3}(\mu_{i+1},t_{i+1})}\neq\frac{Q_{k_2,2}(\mu_{i+1},t_{i+1})}{Q_{k_2,3}(\mu_{i+1},t_{i+1})}$, then the set S_{ai} defined by (85) would be a singleton.

Moreover, since S_i is not a singleton, the definition (84) implies

$$Q_{n,2}(\mu_{i+1},t_{i+1})^2=Q_{n,1}(\mu_{i+1},t_{i+1})Q_{n,3}(\mu_{i+1},t_{i+1}) \tag{87}$$

for all $n\in\mathbb{N}^*$ by recalling (56). According to (59)–(61), and the fact that the Cauchy–Schwarz inequality holds as equality only when two functions are linearly dependent, we obtain the existence of constants $\breve\mu_n$ such that

$$g_{n,1}(t,\mu_{i+1})=\breve\mu_n g_{n,2}(t,\mu_{i+1}),\ n\in\mathbb{N}^* \tag{88}$$

for $t\in[\mu_{i+1},t_{i+1}]$ ($g_{n,2}(t,\mu_{i+1})$ are not identically zero on $t\in[\mu_{i+1},t_{i+1}]$ because $\zeta(t)$ is not identically zero).

Recalling (86), we obtain from (59)–(61) and (88) that

$$g_{n,1}(t,\mu_{i+1})=\overline{\mu}g_{n,2}(t,\mu_{i+1}),\ \overline{\mu}\neq0,\ n\in\mathbb{N}^* \tag{89}$$

for $t\in[\mu_{i+1},t_{i+1}]$. The reason of the constant $\overline{\mu}\neq0$ is given as follows. According to Lemma 3, there exists $n_1\in\mathbb{N}^*$ such that $Q_{n_1,1}(\mu_{i+1},t_{i+1})\neq0$. Hence, $g_{n_1,1}(t,\mu_{i+1})$ is not identically zero on $[\mu_{i+1},t_{i+1}]$.

Equation (89) holding is a necessary condition of the hypothesis that S_i is not a singleton. Recalling (51), (52), and Proposition 1, the fact that the (89) holds implies

$$\int_0^1\sin(x\pi n)u(x,t)dx+\frac{1}{b}\overline{\mu}\varepsilon\pi n\zeta(t)=0 \tag{90}$$

for all $n\in\mathbb{N}^*$, $t\in(\mu_{i+1},t_{i+1})$, and $x\in[0,1]$. Taking the time derivative of (90), and recalling (1) and (2), we have that

$$\begin{aligned}&\int_0^1\sin(x\pi n)(\varepsilon u_{xx}(x,t)+\lambda u(x,t))dx\\&\quad+\frac{1}{b}\overline{\mu}\varepsilon\pi n(a\zeta(t)+bu(0,t))\\&=-(-1)^n\pi n\varepsilon u(1,t)+\pi n\varepsilon u(0,t)\\&\quad-\int_0^1\pi^2n^2\sin(x\pi n)\varepsilon u(x,t)dx\\&\quad+\int_0^1\sin(x\pi n)\lambda u(x,t)dx+\frac{1}{b}\overline{\mu}\varepsilon\pi na\zeta(t)+\overline{\mu}\varepsilon\pi nu(0,t)\\&=-(-1)^n\pi n\varepsilon u(1,t)+n(\pi\varepsilon+\overline{\mu}\varepsilon\pi)u(0,t)\end{aligned}$$

$$-\frac{1}{b}\overline{\mu}\varepsilon\pi n(\lambda - a - \pi^2 n^2\varepsilon)\zeta(t)$$
$$= -(-1)^n\pi\varepsilon u(1,t) + (\pi\varepsilon + \overline{\mu}\varepsilon\pi)u(0,t)$$
$$-\frac{1}{b}\overline{\mu}\varepsilon\pi(\lambda - a - \pi^2 n^2\varepsilon)\zeta(t) = 0 \tag{91}$$

for all $n \in \mathbb{N}^*$ and $t \in (\mu_{i+1}, t_{i+1})$, where (90) is applied in going from the second equation to the third one in (91). Considering any two odd (or even) positive integers $n_1 \neq n_2$, we obtain from (91) that $(n_1^2 - n_2^2)\zeta(t) = 0$ for $t \in (\mu_{i+1}, t_{i+1})$. Considering the fact that $\zeta \in C^0([t_i, t_{i+1}]; \mathbb{R})$ and $\zeta(t)$ is not identically zero on $t \in [t_i, t_{i+1}]$, one obtains $n_1^2 = n_2^2$: contradiction. Consequently, S_i is a singleton, i.e., $S_i = \{(\lambda, a)\}$. Therefore, $\hat{\lambda}(t_{i+1}) = \lambda, \hat{a}(t_{i+1}) = a$. ■

From Claims 1–4, we obtain Lemma 4. ■

Lemma 5: If $\hat{\lambda}(t_i) = \lambda$ (or $\hat{a}(t_i) = a$) for certain $i \in \mathbb{N}$, then $\hat{\lambda}(t) = \lambda$ (or $\hat{a}(t) = a$) for all $t \in [t_i, +\infty)$.

Proof: According to Lemma 4, we have that $\hat{\lambda}(t_{i+1})$ is equal to either λ or $\hat{\lambda}(t_i)$. Therefore, if $\hat{\lambda}(t_i) = \lambda$, then $\hat{\lambda}(t_{i+1}) = \lambda$. Repeating the above process, then $\hat{\lambda}(t) = \lambda$ for all $t \in [t_i, \lim_{k\to\infty}(t_k))$. Recalling Lemma 2 which implies $\lim_{k\to\infty}(t_k) \to \infty$, we thus have $\hat{\lambda}(t) = \lambda$ for $t \in [t_i, \infty)$. The same is true of $\hat{a}$. The proof is complete. ■

Lemma 6: If $u[0] = 0, \zeta(0) \neq 0$, and the user-selected initial estimates $\hat{\theta}(0) = [\hat{\lambda}(0), \hat{a}(0)]^T$ happen to make $K_2(1; \hat{\theta}(0)) = K_2(1; \hat{\theta}(t_1)) = 0$, the situation (i.e., $K_2(1; \hat{\theta}(0)) = K_2(1; \hat{\theta}(t_1)) = 0$) is avoided just by changing $\hat{\lambda}(0)$ as another value (arbitrary) in $[\underline{\lambda}, \overline{\lambda}]$.

Proof: Because the kernels h and γ in K_2 (34) only include the unknown parameter: a, considering $\hat{a}(t_1) = a$ ensured by $\zeta(0) \neq 0$ with Lemma 4, and $\hat{\lambda}(t_1) = \hat{\lambda}(0)$ due to the fact that $u[t]$ is identically zero on $t \in [0, t_1]$ (which is the result of $K_2(1; \hat{\theta}(0)) = 0$ with (1)–(3), (36), (38), and $u[0] = 0$), we have that $K_2(1; \hat{\theta}(t_1)) = K_2(1; \hat{\lambda}(t_1), \hat{a}(t_1)) = K_2(1; \hat{\lambda}(0), a) = K_2(1; \theta) + \frac{\lambda - \hat{\lambda}(0)}{2\varepsilon}\gamma(1)$. Thus $K_2(1; \hat{\theta}(t_1)) = 0$ implies a unique $\hat{\lambda}(0) = \lambda + \frac{2\varepsilon K_2(1;\theta)}{\gamma(1)}$ that is a necessary condition of $K_2(1; \hat{\theta}(0)) = K_2(1; \hat{\theta}(t_1)) = 0$ when $u[0] = 0, \zeta(0) \neq 0$. In other words, if the situation in this lemma appears, it means that $\hat{\lambda}(0)$ must be the one mentioned above. Therefore, we only need to pick another $\hat{\lambda}(0)$, and then the situation mentioned in this lemma is avoided. The proof of Lemma 6 is complete. ■

Remark 1: If $u[0] = 0, \zeta(0) \neq 0$, and $K_2(1; \hat{\theta}(0)) = K_2(1; \hat{\theta}(t_1)) = 0$ is found under the user-selected initial estimates $\hat{\theta}(0) = [\hat{\lambda}(0), \hat{a}(0)]^T$, then $\hat{\lambda}(0)$ should be changed as another value (arbitrary) in $[\underline{\lambda}, \overline{\lambda}]$.

According to Lemma 6, the purpose of Remark 1 is to avoid the appearance of an extreme case that $u[0] = 0$, $\zeta(0) \neq 0$, $K_2(1; \hat{\theta}(0)) = K_2(1; \hat{\theta}(t_1)) = 0$, which implies $K_2(1; \hat{\theta}(t)) = K_2(1; \hat{\theta}(t_1)) = K_2(1; \hat{\lambda}(0), a) = 0$ for $t \geq t_1$, and leads to that the regulation on the ODE dynamics (1) is lost, i.e., $u[t] \equiv 0$ for all time while $\zeta(t)$ dynamics may be unstable, according to (1)–(3), (36), and (38).

Let $\hat{\theta}(0)$ belong to Θ_1 which is equal to Θ together with Remark 1, we obtain the following parameter convergence property.

Relaying on the above four lemmas, we are now to show the convergence of the parameter estimates.

Lemma 7: For all $u[0] \in L^2(0,1)$, $\zeta(0) \in \mathbb{R}$ except for the case that both $u[0]$ and $\zeta(0)$ are zero, with $\hat{\theta}(0) \in \Theta_1$, we have

$$\hat{\theta}(t) = \theta \tag{92}$$

for all $t \geq t_2$, where $\hat{\theta}(t) = [\hat{\lambda}(t), \hat{a}(t)]^T$ and $\theta = [\lambda, a]^T$.

Proof: Case 1: $u(x, 0)$ is not identically zero for $x \in [0, 1]$, and $\zeta(0)$ is not zero. We know that $u[t], \zeta(t)$ are not identically zero on $t \in [0, t_1]$. Recalling Lemmas 4 and 5, we obtain (92).

Case 2: $u[0] = 0$ and $\zeta(0) \neq 0$.

We know that $\zeta(t)$ is not identically zero on $t \in [0, t_1]$. If $K_2(1; \hat{\lambda}(0), \hat{a}(0)) \neq 0$, we have that $u[t]$ is not identically zero on $t \in [0, t_1]$ according to (1)–(3), (36), and (38). Then, it is straightforward to obtain (92) with recalling Lemmas 4 and 5.

If $K_2(1; \hat{\lambda}(0), \hat{a}(0)) = 0$, then $u[t] = 0$ on $t \in [0, t_1]$ according to (1)–(3), (36), (38), and $u[0] = 0$. It follows that $\zeta(t) = \zeta(0)e^{at}$ in (1), which is not zero on $t \in [0, t_1]$ under $\zeta(0) \neq 0$. Recalling Lemma 6 and Remark 1, we have $K_2(1; \hat{\theta}(t_1)) \neq 0$, which results in that $u[t]$ is not identically zero on $t \in [t_1, t_2]$ considering (1)–(3), (36), (38), and the fact that $\zeta(t_1) = \zeta(0)e^{at_1}$ is not zero. Therefore, we obtain (92) from Lemmas 4 and 5.

Case 3: $u(x, 0)$ is not identically zero, and $\zeta(0) = 0$.

It is obvious that $u[t]$ is not identically zero on $t \in [0, t_1]$. Supposing that $\zeta[t]$ is identically zero on $t \in [0, t_1]$, it follows from (1) that $u(0, t) = 0$ on $t \in [0, t_1]$. Applying the method of separation of variables shown in [32, (3.4)–(3.10)], it implies from (2), (3), and $u(0, t) = 0$ that $u[t]$ is identically zero on $t \in [0, t_1]$: contradiction. Therefore, $\zeta[t]$ is also not identically zero on $t \in [0, t_1]$. We thus obtain (92) from Lemmas 4 and 5.

The proof of this lemma is complete. ■

Lemma 7 implies that the exact parameter identification of the two unknown parameters can be achieved by at most two updates of the designed identifier, under all initial conditions of plant states except for a set of measure zero. Because of

$$t_2 \leq 2T \tag{93}$$

which is ensured by (42) we have that the maximum convergence time of the parameter estimates is $2T$, where $T > 0$ is a design parameter.

When all plant initial conditions are zero, the convergence of parameter estimates is shown as the following lemma.

Lemma 8: If $u[0] = 0, \zeta(0) = 0$, the parameter estimates are kept as the initial values, i.e., $\hat{\theta}(t) \equiv \hat{\theta}(0)$ for $t \in [0, \infty)$.

Proof: It is straightforwardly obtained (step by step) from Lemma 4 that $\hat{\theta}(t) \equiv \hat{\theta}(0)$ for $t \in [0, \lim_{i\to\infty} t_i)$. Recalling Lemma 2 that implies $\lim_{i\to\infty} t_i = +\infty$, the proof is complete. ■

Based on Lemmas 7 and 8 showing the convergence of the parameter estimates under different initial conditions $u[0], \zeta(0)$, next we prove the last two portions of Theorem 1 by using Lyapunov analysis.

C. Exponential Regulation of the Plant States

1) Now We Prove the Second Portion of Theorem 1: Define a Lyapunov function as

$$V(t) = \frac{1}{2}r_a\int_0^1 \beta(x,t)^2 dx + \frac{1}{2}r_c\zeta(t)^2 - m(t) \tag{94}$$

where $m(t)$ is defined in (43). Defining

$$\bar{\Omega}(t) = \|\beta[t]\|^2 + \zeta(t)^2 + |m(t)| \quad (95)$$

we have

$$\xi_3\bar{\Omega}(t) \le V(t) \le \xi_4\bar{\Omega}(t) \quad (96)$$

where

$$\xi_3 = \min\left\{\frac{1}{2}r_a, \frac{1}{2}r_c, 1\right\} > 0, \xi_4 = \max\left\{\frac{1}{2}r_a, \frac{1}{2}r_c, 1\right\} > 0.$$

According to (68) and the nominal control design in Section III, in the triggered control system, the right boundary condition of the target system (23)–(26) becomes

$$\beta_x(1,t) + r\beta(1,t) = -p(t) - d(t). \quad (97)$$

Recalling the regularity of the solution in Proposition 1 and the transformations (6), (14), (22), for $t \in (t_i, t_{i+1})$, $i \in \mathbb{N}$, taking the derivative of (94) along (23)–(25), (97), and (43), applying integration by parts, we have that

$$\begin{aligned}\dot{V}(t) &= r_a\int_0^1 \beta(x,t)\beta_t(x,t)dx + r_c\zeta(t)\dot{\zeta}(t) - \dot{m}(t)\\ &= r_a\varepsilon\beta(1,t)(-r\beta(1,t) - p(t) - d(t))\\ &\quad - r_a\varepsilon\int_0^1 \beta_x(x,t)^2dx - a_{\rm m}r_c\zeta(t)^2 + r_c\zeta(t)b\beta(0,t)\\ &\quad + \eta m(t) - \lambda_d d(t)^2 + \kappa_1 u(1,t)^2 + \kappa_2 u(0,t)^2\\ &\quad + \kappa_3\|u(\cdot,t)\|^2 + \kappa_4\zeta(t)^2, \quad t \in (t_i, t_{i+1}). \end{aligned} \quad (98)$$

Recalling (12), (14), and (35), we have

$$\begin{aligned}u(x,t) &= \beta(x,t) - \int_0^x h^I(x,y)\beta(y,t)dy + \gamma(x)\zeta(t)\\ &\quad + \int_0^x \Phi(x,y)\bigg(\beta(y,t) - \int_0^y h^I(y,z)\\ &\quad \times \beta(z,t)dz + \gamma(y)\zeta(t)\bigg)dy\\ &= \beta(x,t) + \int_0^x P(x,y)\beta(y,t)dy + \Gamma(x)\zeta(t) \end{aligned} \quad (99)$$

where

$$P(x,y) = -\int_y^x \Phi(x,z)h^I(z,y)dz - h^I(x,y) + \Phi(x,y)$$

$$\Gamma(x) = \gamma(x) + \int_0^x \Phi(x,y)\gamma(y)dy.$$

Applying the Cauchy–Schwarz inequality, we obtain

$$u(0,t)^2 \le m_1(\beta(0,t)^2 + \zeta(t)^2) \quad (100)$$

$$u(1,t)^2 \le m_2(\beta(1,t)^2 + \zeta(t)^2 + \|\beta[t]\|^2) \quad (101)$$

$$\|u[t]\|^2 \le m_3(\zeta(t)^2 + \|\beta[t]\|^2) \quad (102)$$

where

$$m_1 = 2\max\left\{1, \max_{\vartheta\in\Theta}\{\Gamma(0;\vartheta)^2\}\right\} > 0$$

$$m_2 = 3\max_{\vartheta\in\Theta}\left\{1, \int_0^1 P(1,y;\vartheta)^2dy, \Gamma(1;\vartheta)^2\right\} > 0$$

$$m_3 = 2\max_{\vartheta\in\Theta}\left\{\left(1 + \left(\int_0^1\int_0^x P(x,y;\vartheta)^2dydx\right)^{\frac{1}{2}}\right)^2,\right.$$
$$\left.\int_0^1 \Gamma(x;\vartheta)^2dx\right\} > 0.$$

From Poincare inequality, we have that

$$-\|\beta_x[t]\|^2 \le \frac{1}{2}\beta(1,t)^2 - \frac{1}{4}\|\beta[t]\|^2. \quad (103)$$

From Agmon's and Young's inequalities, we have that

$$\beta(0,t)^2 \le \beta(1,t)^2 + \|\beta[t]\|^2 + \|\beta_x[t]\|^2. \quad (104)$$

Applying Young's inequality and the Cauchy–Schwarz inequality into (98), with using (100)–(102), (103), and (104), we have that

$$\begin{aligned}\dot{V}(t) \le &-rr_a\varepsilon\beta(1,t)^2 - r_a\varepsilon\beta(1,t)p(t) - r_a\varepsilon\beta(1,t)d(t)\\ &- \frac{1}{8}r_a\varepsilon\int_0^1 \beta(x,t)^2dx + \frac{1}{4}r_a\varepsilon\beta(1,t)^2\\ &- \frac{1}{2}r_a\varepsilon\int_0^1 \beta_x(x,t)^2dx - \frac{3}{4}a_{\rm m}r_c\zeta(t)^2 + \frac{r_c}{a_{\rm m}}b^2\beta(0,t)^2\\ &+ \eta m(t) - \lambda_d d(t)^2 + \kappa_1 m_2\beta(1,t)^2 + \kappa_2 m_1\beta(0,t)^2\\ &+ (\kappa_3 m_3 + \kappa_1 m_2)\|\beta(\cdot,t)\|^2\\ &+ (\kappa_4 + \kappa_2 m_1 + \kappa_1 m_2 + \kappa_3 m_3)\zeta(t)^2\\ \le &-\bigg[\left(r - \frac{1}{4}\right)r_a\varepsilon - \frac{r_a\varepsilon}{4r_1} - \frac{r_a\varepsilon}{4r_2} - \frac{r_c}{a_{\rm m}}b^2\\ &- \kappa_1 m_2 - \kappa_2 m_1\bigg]\beta(1,t)^2\\ &+ \eta m(t) - (\lambda_d - r_1 r_a\varepsilon)d(t)^2 + r_2 r_a\varepsilon p(t)^2\\ &- \left(\frac{3r_c}{4}a_{\rm m} - \kappa_1 m_2 - \kappa_2 m_1 - \kappa_3 m_3 - \kappa_4\right)\zeta(t)^2\\ &- \left(\frac{1}{2}r_a\varepsilon - \frac{r_c}{a_{\rm m}}b^2 - \kappa_2 m_1\right)\|\beta_x[t]\|^2\\ &- \left(\frac{1}{8}r_a\varepsilon - \frac{r_c}{a_{\rm m}}b^2 - \kappa_1 m_2 - \kappa_2 m_1 - \kappa_3 m_3\right)\|\beta[t]\|^2 \end{aligned}$$

for $t \in (t_i, t_{i+1})$. Choosing

$$\min\{r_1, r_2\} \ge \frac{1}{q - \frac{\bar{\lambda}}{2\varepsilon} - \frac{1}{4}} \ge \frac{1}{r - \frac{1}{4}} \quad (105)$$

$$r_c > \frac{8(\kappa_1 m_2 + \kappa_2 m_1 + \kappa_3 m_3 + \kappa_4)}{3a_{\rm m}} \quad (106)$$

$$r_a \ge \max\left\{\frac{2(\frac{r_c}{a_m}b^2 + \kappa_1 m_2 + \kappa_2 m_1)}{(q - \frac{\bar{\lambda}}{2\varepsilon} - \frac{1}{4})\varepsilon}, \frac{2}{\varepsilon}\left(\frac{r_c}{a_{\rm m}}b^2 + \kappa_2 m_1\right)\right.$$
$$\left.\frac{16(\frac{r_c}{a_{\rm m}}b^2 + \kappa_1 m_2 + \kappa_2 m_1 + \kappa_3 m_3)}{\varepsilon}\right\} \quad (107)$$

$$\lambda_d \ge r_1 r_a\varepsilon \quad (108)$$

where $r = q - \frac{\lambda}{2\varepsilon}$ in (27) and Assumption 2, which ensures $r \geq q - \frac{\bar{\lambda}}{2\varepsilon} > \frac{1}{4}$ are recalled, we obtain

$$\dot{V} \leq -\frac{1}{16} r_a \varepsilon \|\beta[t]\|^2 - \frac{3r_c}{8} a_{\mathrm{m}} \zeta(t)^2 + \eta m(t) + r_2 r_a \varepsilon p(t)^2. \tag{109}$$

That is,

$$\dot{V} \leq -\sigma V(t) + r_2 r_a \varepsilon p(t)^2 \tag{110}$$

for $t \in (t_i, t_{i+1})$, $i \in \mathbb{N}$, where

$$\sigma = \min\left\{\frac{1}{8}\varepsilon, \frac{3}{4}a_{\mathrm{m}}, \eta\right\}.$$

Claim 5: After $t = t_2$, $p(t)$ defined in (41) is identically zero, i.e.,

$$p(t) \equiv 0, \ t \in [t_2, \infty). \tag{111}$$

Proof: 1) If $u[0]$ and $\zeta(0)$ are zero, it follows that $u[t]$ and $\zeta(t)$ are identically zero for $t \in [0, \infty)$ considering (1)–(3), (36), and (38). Thus, (111) holds.

2) Others: Recalling (41) and Lemma 7, we obtain (111).

The proof of Claim 5 is complete. ■

Multiplying both sides of (110) by $e^{\sigma t}$, integrating both sides of (110) from t_i to t with $t \in (t_i, t_{i+1})$, $i \geq 2$, considering Claim 5, we obtain that

$$V(t) \leq V(t_i) e^{-\sigma(t - t_i)}, \ t \in (t_i, t_{i+1}), \ i \geq 2. \tag{112}$$

Recalling Corollary 1, we know that $V(t)$ defined in (94) is continuous. We then have $V(t_{i+1}^-) = V(t_{i+1})$ and $V(t_i^+) = V(t_i)$, and thus, we can replace (t_i, t_{i+1}) by $[t_i, t_{i+1}]$ in (112), yielding

$$V(t_{i+1}) \leq V(t_i) e^{-\sigma(t_{i+1} - t_i)} \tag{113}$$

for $i \geq 2$.

Hence, applying (113) repeatedly, we obtain from (112) that

$$V(t) \leq V(t_2) \prod_{c=2}^{i-1} e^{-\sigma(t_{c+1} - t_c)} e^{-\sigma(t - t_i)} = V(t_2) e^{-\sigma(t - t_2)} \tag{114}$$

for any $t \in [t_i, t_{i+1}]$, $i \geq 3$. Together with (112) holding for $t \in [t_2, t_3]$, we obtain

$$V(t) \leq V(t_2) e^{-\sigma(t - t_2)} \tag{115}$$

for $t \geq t_2$.

In the following claim, we analyze the responses on $t \in [0, t_2]$.

Claim 6: For the finite time t_2 in Claim 5, the following estimate holds:

$$V(t) \leq V(0) e^{\bar{\sigma} t}, \ t \in [0, t_2] \tag{116}$$

where

$$\bar{\sigma} = \frac{1}{\xi_3} \max\{r_2 r_a \varepsilon \Upsilon_p, 1\} - \min\left\{\frac{1}{8}\varepsilon, \frac{3}{4}a_{\mathrm{m}}, \eta + 1\right\} \tag{117}$$

for some positive Υ_p that depends on the initial parameter estimates $\hat{\lambda}(0)$ and $\hat{a}(0)$ and its true values λ and a.

Proof: Bounding $p(t)^2$ defined in (41) on $t \in [0, t_2]$ as

$$p(t)^2 \leq \bar{\Upsilon}_p (\|u[t]\|^2 + \zeta(t)^2)$$

with

$$\bar{\Upsilon}_p = 2 \max\left\{ \int_0^1 (K_1(1, y; \lambda, a) - K_1(1, y; \hat{\lambda}, \hat{a}))^2 dy, (K_2(1; \lambda, a) - K_2(1; \hat{\lambda}, \hat{a}))^2 \right\} \tag{118}$$

where $\hat{\lambda}$ is equal to $\hat{\lambda}(0)$ or λ, $\hat{a}$ is equal to $\hat{a}(0)$ or a, because only $\hat{\lambda}(0), \hat{a}(0)$ and $\hat{\lambda}(t_1), \hat{a}(t_1)$ are used here, with recalling Lemma 4 that implies that $\hat{\lambda}(t_1) = \lambda$ or $\hat{\lambda}(t_1) = \hat{\lambda}(0)$ and $\hat{a}(t_1) = a$ or $\hat{a}(t_1) = \hat{a}(0)$. Recalling (102), we obtain

$$p(t)^2 \leq \Upsilon_p (\|\beta[t]\|^2 + \zeta(t)^2), \ t \in [0, t_2] \tag{119}$$

where the positive constant Υ_p is

$$\Upsilon_p = \bar{\Upsilon}_p (m_3 + 1). \tag{120}$$

For $0 \leq i < 2$, we have from (109) and (119) that

$$\dot{V}(t) \leq -\frac{1}{16} r_a \varepsilon \|\beta[t]\|^2 - \frac{3r_c}{8} a_{\mathrm{m}} \zeta(t)^2 + \eta m(t) + m(t) - m(t) + r_2 r_a \varepsilon \Upsilon_p (\|\beta[t]\|^2 + \zeta(t)^2) \leq \bar{\sigma} V(t)$$

for $t \in (t_i, t_{i+1})$, where $\bar{\sigma}$ is given in (117). We then have

$$V(t) \leq V(t_i) e^{\bar{\sigma}(t - t_i)} \tag{121}$$

for $t \in (t_i, t_{i+1}), 0 \leq i < 2$. Recalling again the continuity of $V(t)$, and thus, we can replace (t_i, t_{i+1}) by $[t_i, t_{i+1}]$ in (121).

Then, we have

$$V(t_1) \leq V(0) e^{\bar{\sigma} t_1}. \tag{122}$$

Recalling (121) and applying (122), we have that

$$V(t) \leq V(0) e^{\bar{\sigma} t_1} e^{\bar{\sigma}(t - t_1)} = V(0) e^{\bar{\sigma} t}$$

for any $t \in [t_1, t_2]$. It is obtained from (121) that $V(t) \leq V(0) e^{\bar{\sigma} t}$ also holds for $t \in [0, t_1]$. Therefore, (116) holds.

The proof of Claim 6 is complete. ■

We obtain from Claim 6 that

$$V(t_2) \leq V(0) e^{\bar{\sigma} t_2}. \tag{123}$$

By virtue of (115), (116), and (123), we have $V(t) \leq V(0) e^{(\bar{\sigma} + \max\{\sigma, -\bar{\sigma}\}) t_2} e^{-\sigma t} \leq V(0) e^{2T(\bar{\sigma} + \max\{\sigma, -\bar{\sigma}\})} e^{-\sigma t}$ for $t \in [0, \infty)$, where (93) is recalled. Recalling (96), we have

$$\bar{\Omega}(t) \leq \Upsilon_1 \bar{\Omega}(0) e^{-\sigma t}, t \geq 0 \tag{124}$$

where the positive constant Υ_1 is

$$\Upsilon_1 = \frac{\xi_4}{\xi_3} e^{2T(\bar{\sigma} + \max\{\sigma, -\bar{\sigma}\})} \tag{125}$$

which depends on the initial parameter estimates $\hat{\lambda}(0)$ and $\hat{a}(0)$ recalling (117), (118), and (120).

From (5), (37), and Lemma 7, we know that $\tilde{\theta}(t) = 0 \, \forall t \geq t_2$, and $|\tilde{\theta}(t)| \leq |\tilde{\theta}(0)| \, \forall t \in [0, t_2]$, which is ensured by Lemma 4. Recalling (93), the following estimate holds: $|\tilde{\theta}(t)| \leq e^{2\sigma T} |\tilde{\theta}(0)| e^{-\sigma t}$. Therefore, together with (124), we have that

$$\left(\bar{\Omega}(t) + \left|\tilde{\theta}(t)\right|\right) \leq \Upsilon \left(\bar{\Omega}(0) + \left|\tilde{\theta}(0)\right|\right) e^{-\sigma t} \tag{126}$$

where

$$\Upsilon = \max\{\Upsilon_1, e^{2\sigma T}\}.$$

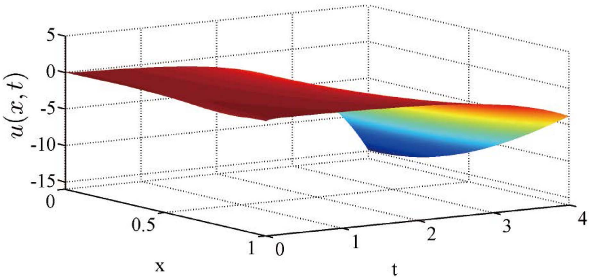

Fig. 3. Evolution of $u(x,t)$ in an open loop.

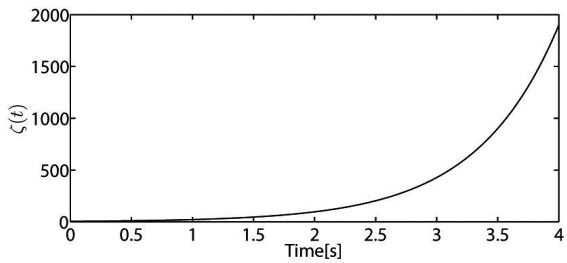

Fig. 4. Evolution of $\zeta(t)$ in an open loop.

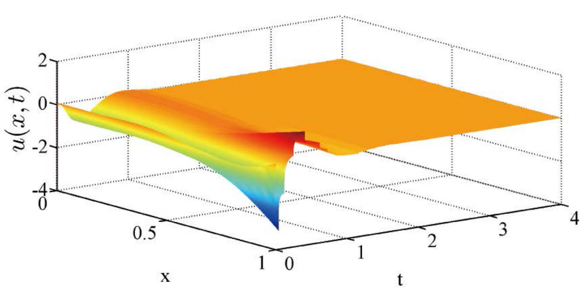

Fig. 5. Evolution of $u(x,t)$ under the control input $U_d(t)$ defined in (36).

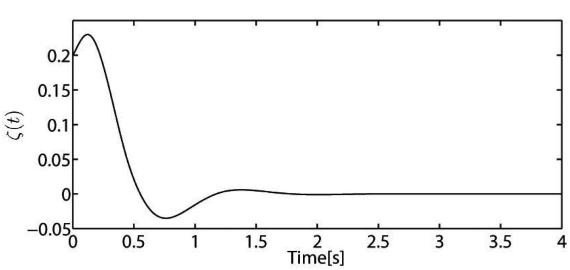

Fig. 6. Evolution of $\zeta(t)$ under the control input $U_d(t)$ defined in (36).

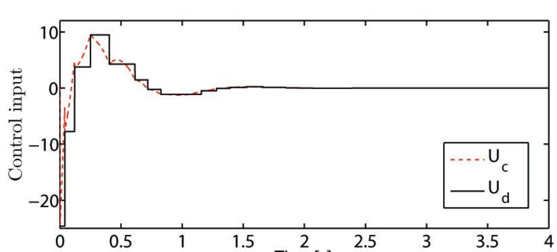

Fig. 7. Piecewise-constant control input $U_d(t)$ (36) and the continuous-in-state control signal $U_c(t)$ (39) used in ETM.

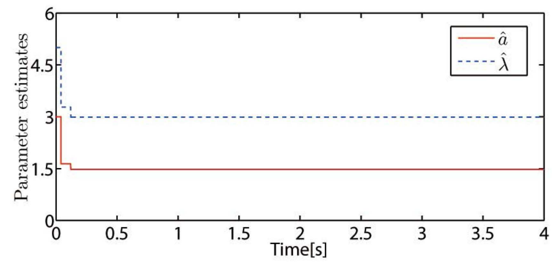

Fig. 8. Evolution of the parameter estimates.

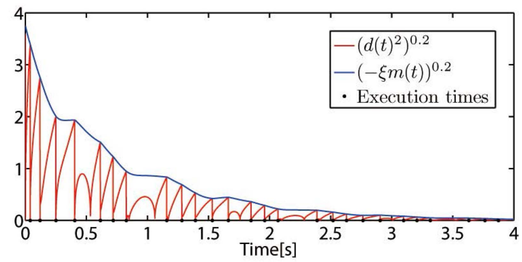

Fig. 9. Evolution of $(d(t)^2)^{0.2}$ and $(-\xi m(t))^{0.2}$.

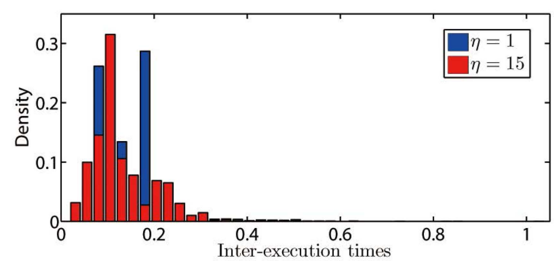

Fig. 10. Density of the inter-execution times computed for 100 different initial conditions given by $u(x,0) = x^2 \sin(\bar{n}\pi x)$, $\zeta(0) = 0.2$, and $\bar{n} = 1, 2, \ldots, 100$.

Applying the invertibility of the transformations (6), (14), and (22), we thus obtain (64).

2) Now We Prove the Last Portion of Theorem 1: It follows from (1)–(3), (36), (38), and $u[0] = 0, \zeta(0) = 0$ that $u[t] \equiv 0$ and $\zeta(t) \equiv 0$ for $t \in [0, \infty)$. Recalling (40) and (43), we know $m(t) = m(0)e^{-\eta t}$, i.e., $|m(t)| \leq |m(0)|$, for $t \in [0, \infty)$. Also, it is obtained from Lemma 8 that $\tilde{\theta}(t) \equiv \theta - \hat{\theta}(0)$ for $t \in [0, \infty)$. Therefore, (65) is obtained.

The proof of Theorem 1 is complete.

VI. Simulation

A. Model

The simulation model is (1)–(4) with the following parameters: $a = 1.5$, $b = 1$, $\varepsilon = 1$, $\lambda = 3$, and $q = 5$. The bounds $\overline{\lambda}, \underline{\lambda}, \overline{a}$, and $\underline{a}$ of the unknown parameters λ and a are set as $0, 5, 0,$ and 3, respectively. Initial conditions are defined as

$$u(x,0) = x^2 \sin(2\pi x), \ \zeta(0) = 5. \tag{127}$$

In the numerical calculation by the finite difference method, the model is discretized with the time step of 0.004 and the space step of 0.05.

B. Design Parameters

The design parameters are chosen as $\xi = 1.1$, $\tilde{N} = 5$, $T = 1.2$, $\eta = 15$, $\kappa = 16$, $\kappa_1 = \kappa_2 = \kappa_3 = \kappa_4 = 100$, $\lambda_d = 20$, and n in (62) is truncated at 15 and the initial condition of $m(t)$ is set as $m(0) = -500$. The function of free design parameters $\tilde{N}$, T, η, ξ, and $m(0)$ in adjusting the response of the closed-loop system is illustrated as follows. A larger $m(0)$ can reduce the triggering times at the initial stage, which allows more data being collected for least-squares parameter identification. Even though a larger overshoot of the plant norms may appear due to the large $m(0)$, the increase of η can fasten the convergence of $m(t)$ to zero, together with the decrease of ξ, which can make the plant states resampled more frequently, especially after the parameter estimates reaching the true values (which can always be achieved in initial several updates), and thus increase the decay rate of the plant states. Besides, as mentioned, when we introduce the design parameters $\tilde{N}, T$, the increase of $\tilde{N}$ allows the data in more time intervals to be used in parameter identification, which can improve the accuracy and robustness of the identifier, and T is chosen to avoid less frequent updates of parameter estimates considering the operation time is only 4 s.

C. Gain Kernels

The kernels $\lambda(x)$, $\Psi(x, y)$ are directly obtained from (15) and (7) (using the modified Bessel function given in [32, (A.10)] with $n = 1$ and cutting off m in [32, (A.10)] at 15), where the unknown coefficients are replaced by the piecewise-constant estimates. The approximate solution $h(x, y)$ of (28)–(31) where the unknown coefficients are replaced by the piecewise-constant estimates is obtained by the finite difference method on a lower triangular domain discretized as a grid with the uniformed interval of 0.05 (the spatial variables x and y were discretized using 21 grid points each). The value at each grid point is denoted as $h_{i,j}$, $1 \le j \le i \le 21, i, j \in 1, 2, \ldots, 21$. According to (31), we know $h_{1,1} = 0$. Together with (30), we have $h_{i,i} = 0, i = 1, 2, \ldots, 21$. Then, $h_{2,1}$ can be solved via (28). For representing the two-order derivatives in (29) by the finite difference scheme, we adopt the following approximate $h_{i,i-1} = h_{2,1}, i = 2, \ldots, 21$. The kernel h will be recomputed when the parameter estimates are changed in the evolution. In the simulation results, which will be shown later, we know that h is recomputed twice, according to the parameter estimates $\hat{\lambda}$ and $\hat{a}$.

D. Simulation Results

The open-loop response of the ODE state $\zeta(t)$ and PDE state $u(x, t)$ are shown in Figs. 3 and 4, from which we observe that the plant is unstable. Applying the proposed adaptive event-triggered controller U_d defined in (36), it is shown in Figs. 5 and 6 that the ODE state $\zeta(t)$ and PDE state $u(x, t)$ are convergent to zero. The piecewise-constant control input $U_d(t)$ defined in (36) and the continuous-in-state control signal $U_c(t)$ (39) used in ETM are shown in Fig. 7. For the control input $U_d(t)$, the estimate $\hat{\theta}$ is recomputed and the states u and ζ are resampled simultaneously, the total number of triggering times is 26, the minimal dwell-time is 0.0404 s, which is much larger than the highly conservative minimal dwell-time estimate (whose order of magnitude is 10^{-6} s) obtained from (81) and (82) in Lemma 2. There are two "jumps" in the continuous-in-state control signal $U_c(t)$ (39) at the first two triggering times, because of the updates in the parameter estimates, which are shown in Fig. 8, where the estimates reach the true values after two triggering times (the exact estimates are not obtained at the time of the first event under the nonzero initial condition (127) as Lemmas 4 and 5 imply, because of the approximation adopted in the simulation, including the discretization of time and space, and truncation of $n = 1, 2, \ldots$ in the estimator (62)).

Fig. 9 shows the time evolution of the functions in the triggering condition (42) and the execution times, where an event is generated, the control value is updated and $d(t)$ is reset to zero, when the trajectory $d(t)^2$ reaches the trajectory $-\xi m(t)$.

Finally, we run simulations for 100 different initial conditions and compute the inter-execution times between two triggering times. The density of the inter-execution times is shown in Fig. 10, from which we know that the prominent inter-execution times are around 0.1 s when $\eta = 15$, and increase to around 0.2 s when η decreases to 1.

VII. Conclusion

In this article, we have proposed an adaptive event-triggered boundary control scheme for a parabolic PDE–ODE system, where the reaction coefficient of the parabolic PDE, and the system parameter of the ODE are unknown, and both of the parameter estimates and control input employ piecewise-constant values. The controller includes an ETM to determine the synchronous update times of both the BaLSI and plant states in the control law. We have proved that the proposed control guarantees that 1) no Zeno phenomenon occurs; 2) parameter estimates are convergent to the true values in finite time under most initial conditions of the plant (all initial conditions of the plant except for a set of measure zero); and 3) the plant states are exponentially regulated to zero. The effectiveness of the proposed design is verified by a numerical example. In the future work, the state-feedback control design will be extended to the output-feedback type conforming to available sensors in practice.

Appendix

A. Calculating Conditions of $\gamma(x)$

Inserting (14) into (16), recalling (8) and (20), we have

$$\begin{aligned}&\dot{\zeta}(t) + a_{\mathrm{m}}\zeta(t) - bw(0, t) + b\gamma(0)\zeta(t)\\&= \dot{\zeta}(t) - a\zeta(t) - bw(0, t) + (b\kappa + b\gamma(0))\zeta(t)\\&= (b\kappa + b\gamma(0))\zeta(t) = 0.\end{aligned} \tag{128}$$

Inserting (14) into (17), recalling (9) and (16), we have

$$\begin{aligned}&v_t(x, t) - \varepsilon v_{xx}(x, t) + \gamma(x) bv(0, t)\\&= w_t(x, t) - \gamma(x)\dot{\zeta}(t) - \varepsilon w_{xx}(x, t)\\&\quad + \varepsilon\gamma''(x)\zeta(t) + \gamma(x) bv(0, t)\\&= \gamma(x) a_{\mathrm{m}}\zeta(t) - \gamma(x) bv(0, t) + \varepsilon\gamma''(x)\zeta(t) + \gamma(x) bv(0, t)\\&= (\gamma(x) a_{\mathrm{m}} + \varepsilon\gamma''(x))\zeta(t) = 0.\end{aligned} \tag{129}$$

By virtue of (18) and (10), we have

$$v_x(0,t) = w_x(0,t) - \gamma'(0)\zeta(t) = -\gamma'(0)\zeta(t) = 0. \quad (130)$$

According to (128)–(130), the conditions of $\gamma(x)$ are obtained as

$$\varepsilon\gamma''(x) + a_{\mathrm{m}}\gamma(x) = 0 \quad (131)$$

$$\gamma(0) = -\kappa \quad (132)$$

$$\gamma'(0) = 0 \quad (133)$$

which are satisfied by (15).

B. Calculating Conditions of $h(x,y)$

Inserting (22) into (24), using (17) and (18), applying integration by parts twice, we obtain

$$\begin{aligned}
&\beta_t(x,t) - \varepsilon\beta_{xx}(x,t)\\
&= v_t(x,t) - \int_0^x h(x,y)v_t(y,t)dy - \varepsilon v_{xx}(x,t)\\
&\quad + \varepsilon\int_0^x h_{xx}(x,y)v(y,t)dy + \varepsilon h_x(x,x)v(x,t)\\
&\quad + \varepsilon h_x(x,x)v(x,t) + \varepsilon h_y(x,x)v(x,t) + \varepsilon h(x,x)v_x(x,t)\\
&= -\gamma(x)bv(0,t) - \int_0^x h(x,y)\varepsilon v_{xx}(y,t)dy\\
&\quad + b\int_0^x h(x,y)\gamma(y)dyv(0,t) + \varepsilon\int_0^x h_{xx}(x,y)v(y,t)dy\\
&\quad + 2\varepsilon h_x(x,x)v(x,t) + \varepsilon h_y(x,x)v(x,t) + \varepsilon h(x,x)v_x(x,t)\\
&= -\gamma(x)bv(0,t) - h(x,x)\varepsilon v_x(x,t) + h(0,0)\varepsilon v_x(0,t)\\
&\quad + h_y(x,x)\varepsilon v(x,t) - h_y(x,0)\varepsilon v(0,t)\\
&\quad - \int_0^x h_{yy}(x,y)\varepsilon v(y,t)dy + b\int_0^x h(x,y)\gamma(y)dyv(0,t)\\
&\quad + \varepsilon\int_0^x h_{xx}(x,y)v(y,t)dy + 2\varepsilon h_x(x,x)v(x,t)\\
&\quad + \varepsilon h_y(x,x)v(x,t) + \varepsilon h(x,x)v_x(x,t)\\
&= -\left(h_y(x,0)\varepsilon + \gamma(x)b - b\int_0^x h(x,y)\gamma(y)dy\right)v(0,t)\\
&\quad + (\varepsilon h(x,x) - h(x,x)\varepsilon)v_x(x,t)\\
&\quad + 2\varepsilon(h_y(x,x) + h_x(x,x))v(x,t)\\
&\quad - \varepsilon\int_0^x (h_{yy}(x,y) - h_{xx}(x,y))v(y,t)dy = 0. \quad (134)
\end{aligned}$$

By virtue of (25) and (18), we have

$$\beta_x(0,t) = v_x(0,t) - h(0,0)v(0,t) = -h(0,0)v(0,t) = 0. \quad (135)$$

According to (134) and (135), we obtain the conditions (28)–(31).

References

[1] T. Ahmed-Ali, F. Giri, M. Krstic, F. Lamnabhi-Lagarrigue, and L. Burlion, "Adaptive observer for a class of parabolic PDEs," *IEEE Trans. Autom. Control*, vol. 61, no. 10, pp. 3083–3090, Oct. 2016.

[2] T. Ahmed-Ali, F. Giri, M. Krstic, L. Burlion, and F. Lamnabhi-Lagarrigue, "Adaptive observer design with heat PDE sensor," *Automatica*, vol. 82, pp. 93–100, 2017.

[3] H. Anfinsen and O. M. Aamo, *Adaptive Control of Hyperbolic PDEs*. Berlin, Germany: Springer, 2019.

[4] M. Bagheri, I. Karafyllis, P. Naseradinmousavi, and M. Krstic, "Adaptive control of a two-link robot using batch least-squares identifier," *IEEE/CCA J. Automatica Sinica*, vol. 8, no. 1, pp. 86–93, Jan. 2021.

[5] A. Baccoli, A. Pisano, and Y. Orlov, "Boundary control of coupled reaction-diffusion processes with constant parameters," *Automatica*, vol. 54, pp. 80–90, 2015.

[6] N. Bekiaris-Liberis and M. Krstic, "Compensating the distributed effect of diffusion and counter-convection in multi-input and multi-output LTI systems," *IEEE Trans. Autom. Control*, vol. 56, no. 3, pp. 637–643, Mar. 2011.

[7] P. Bernard and M. Krstic, "Adaptive output-feedback stabilization of non-local hyperbolic PDEs," *Automatica*, vol. 50, pp. 2692–2699, 2014.

[8] J. Deutscher, "A backstepping approach to the output regulation of boundary controlled parabolic PDEs," *Automatica*, vol. 57, pp. 56–64, 2015.

[9] J. Deutscher, "Backstepping design of robust output feedback regulators for boundary controlled parabolic PDEs," *IEEE Trans. Autom. Control*, vol. 61, no. 8, pp. 2288–2294, Aug. 2016.

[10] J. Deutscher and N. Gehring, "Output feedback control of coupled linear parabolic ODE-PDE-ODE systems," *IEEE Trans. Autom. Control*, vol. 66, no. 10, pp. 4668–4683, Oct. 2021, doi: 10.1109/TAC.2020.3030763.

[11] J. Deutscher and S. Kerschbaum, "Backstepping control of coupled linear parabolic PIDEs with spatially varying coefficients," *IEEE Trans. Autom. Control*, vol. 63, no. 12, pp. 4218–4233, Dec. 2018.

[12] N. Espitia, "Observer-based event-triggered boundary control of a linear 2×2 hyperbolic systems," *Syst. Control Lett.*, vol. 138, 2020, Art. no. 104668.

[13] N. Espitia, A. Girard, N. Marchand, and C. Prieur, "Event-based control of linear hyperbolic systems of conservation laws," *Automatica*, vol. 70, pp. 275–287, 2016.

[14] N. Espitia, A. Girard, N. Marchand, and C. Prieur, "Event-based boundary control of a linear 2×2 hyperbolic system via backstepping approach," *IEEE Trans. Autom. Control*, vol. 63, no. 8, pp. 2686–2693, Aug. 2018.

[15] N. Espitia, I. Karafyllis, and M. Krstic, "Event-triggered boundary control of constant-parameter reaction-diffusion PDEs: A small-gain approach," *Automatica*, vol. 128, 2021, Art. no. 109562.

[16] E. Fridman and A. Blighovsky, "Robust sampled-data control of a class of semilinear parabolic systems," *Automatica*, vol. 48, no. 5, pp. 826–836, 2012.

[17] A. Girard, "Dynamic triggering mechanisms for event-triggered control," *IEEE Trans. Autom. Control*, vol. 60, no. 7, pp. 1992–1997, Jul. 2015.

[18] W. P. M. H. Heemels and M. C. F. Donkers, "Model-based periodic event-triggered control for linear systems," *Automatica*, vol. 49, pp. 698–711, 2013.

[19] W. P. M. H. Heemels, K. H. Johansson, and P. Tabuada, "An introduction to event-triggered and self-triggered control," in *Proc. IEEE 51st Conf. Decis. Control*, 2012, pp. 3270–3285.

[20] I. Karafyllis, M. Kontorinaki, and M. Krstic, "Adaptive control by regulation-triggered batch least squares," *IEEE Trans. Autom. Control*, vol. 65, no. 7, pp. 2842–2855, Jul. 2020.

[21] I. Karafyllis and M. Krstic, "Sampled-data boundary feedback control of 1-D linear transport PDEs with non-local terms," *Syst. Control Lett.*, vol. 107, pp. 68–75, 2017.

[22] I. Karafyllis and M. Krstic, "Adaptive certainty-equivalence control with regulation-triggered finite-time least-squares identification," *IEEE Trans. Autom. Control*, vol. 63, no. 10, pp. 3261–3275, Oct. 2018.

[23] I. Karafyllis and M. Krstic, *Input-to-State Stability for PDEs*. Berlin, Germany: Springer, 2019.

[24] I. Karafyllis, M. Krstic, and K. Chrysafi, "Adaptive boundary control of constant-parameter reaction-diffusion PDEs using regulation-triggered finite-time identification," *Automatica*, vol. 103, pp. 166–179, 2019.

[25] R. Katz, E. Fridman, and A. Selivanov, "Network-based boundary observer-controller design for 1D heat equation," in *Proc. 58th IEEE Conf. Decis. Control*, 2019, pp. 2151–2156.

[26] R. Katz, E. Fridman, and A. Selivanov, "Boundary delayed observer-controller design for reaction-diffusion systems," *IEEE Trans. Autom. Control*, vol. 66, no. 1, pp. 275–282, Jan. 2021.

[27] S. Koga, L. Camacho-Solorio, and M. Krstic, "State estimation for lithium ion batteries with phase transition materials," in *Proc. ASME Dyn. Syst. Control Conf.*, 2017, Art. no. V003T43A002.

[28] S. Koga, M. Diagne, and M. Krstic, "Control and state estimation of the one-phase Stefan problem via backstepping design," *IEEE Trans. Autom. Control*, vol. 64, no. 2, pp. 510–525, Feb. 2019.

[29] M. Krstic, "Systematization of approaches to adaptive boundary stabilization of PDEs," *Int. J. Robust Nonlinear*, vol. 16, pp. 801–818, 2006.

[30] M. Krstic, "Compensating actuator and sensor dynamics governed by diffusion PDEs," *Syst. Control Lett.*, vol. 58, pp. 372–377, 2009.

[31] M. Krstic, I. Kanellakopoulos, and P. Kokotovic, *Nonlinear and Adaptive Control Design*. Hoboken, NJ, USA: Wiley, 1995.

[32] M. Krstic and A. Smyshlyaev, *Boundary Control of PDEs*. Philadelphia, PA, USA: SIAM, 2008.

[33] M. Krstic and A. Smyshlyaev, "Adaptive boundary control for unstable parabolic PDEs—Part I: Lyapunov design," *IEEE Trans. Autom. Control*, vol. 53, no. 7, pp. 1575–1591, Aug. 2008.

[34] J. Li and Y. Liu, "Adaptive control of uncertain coupled reaction-diffusion dynamics with equidiffusivity in the actuation path of an ODE system," *IEEE Trans. Autom. Control*, vol. 66, no. 2, pp. 802–809, Feb. 2021.

[35] W. Liu, "Boundary feedback stabilization of an unstable heat equation," *SIAM J. Control Optim.*, vol. 42, pp. 1033–1042, 2003.

[36] W. Liu and M. Krstic, "Backstepping boundary control of Burgers' equation with actuator dynamics," *Syst. Control Lett.*, vol. 41, pp. 291–303, 2000.

[37] S. Marx, L. Brivadis, and D. Astolfi, "Forwarding techniques for the global stabilization of dissipative infinite-dimensional systems coupled with an ODE," *Math. Control Signals Syst.*, vol. 33, pp. 755–774, 2021.

[38] F. Mazenc and L. Praly, "Adding integrations, saturated controls, and stabilization for feedforward systems," *IEEE Trans. Autom. Control*, vol. 41, no. 11, pp. 1559–1578, Nov. 1996.

[39] T. Meurer and A. Kugi, "Tracking control for boundary controlled parabolic PDEs with varying parameters: Combining backstepping and differential flatness," *Automatica*, vol. 45, pp. 1182–1194, 2009.

[40] Y. Orlov, A. Pisano, A. Pilloni, and E. Usai, "Output feedback stabilization of coupled reaction-diffusion processes with constant parameters," *SIAM J. Control Optim.*, vol. 55, no. 6, pp. 4112–4155, 2017.

[41] B. Petrus, J. Bentsman, and B. G. Thomas, "Enthalpy-based feedback control algorithms for the Stefan problem," in *Proc. IEEE Conf. Decis. Control*, 2012, pp. 7037–7042.

[42] A. Pisano and Y. Orlov, "Boundary second-order sliding-mode control of an uncertain heat process with unbounded matched perturbation," *Automatica*, vol. 48, pp. 1768–1775, 2012.

[43] B. Rathnayake, M. Diagne, N. Espitia, and I. Karafyllis, "Observer-based event-triggered boundary control of a class of reaction-diffusion PDEs," *IEEE Trans. Autom. Control*, vol. 67, no. 6, pp. 2905–2917, Jun. 2022.

[44] A. Selivanov and E. Fridman, "Distributed event-triggered control of diffusion semilinear PDEs," *Automatica*, vol. 68, pp. 344–351, 2016.

[45] A. Seuret, C. Prieur, and N. Marchand, "Stability of non-linear systems by means of event-triggered sampling algorithms," *IMA J. Math. Control Inf.*, vol. 31, no. 3, pp. 415–433, 2014.

[46] A. Smyshlyaev and M. Krstic, "Adaptive boundary control for unstable parabolic PDEs—Part II: Estimation-based designs," *Automatica*, vol. 43, pp. 1543–1556, 2007.

[47] A. Smyshlyaev and M. Krstic, "Adaptive boundary control for unstable parabolic PDEs—Part III: Output feedback examples with swapping identifiers," *Automatica*, vol. 43, pp. 1557–1564, 2007.

[48] G. A. Susto and M. Krstic, "Control of PDE-ODE cascades with Neumann interconnections," *J. Franklin Inst.*, vol. 347, pp. 284–314, 2010.

[49] P. Tabuada, "Event-triggered real-time scheduling of stabilizing control tasks," *IEEE Trans. Autom. Control*, vol. 52, no. 9, pp. 1680–1685, Sep. 2007.

[50] S.-X. Tang and C. Xie, "State and output feedback boundary control for a coupled PDE-ODE system," *Syst. Control Lett.*, vol. 60, pp. 540–545, 2011.

[51] S.-X. Tang, L. Camacho-Solorio, Y. Wang, and M. Krstic, "State-of-charge estimation from a thermal-electrochemical model of lithium-ion batteries," *Automatica*, vol. 83, pp. 206–219, 2017.

[52] A. Tanwani, C. Prieur, and M. Fiacchini, "Observer-based feedback stabilization of linear systems with event-triggered sampling and dynamic quantization," *Syst. Control Lett.*, vol. 94, pp. 46–56, 2016.

[53] A. Terrand-Jeanne, V. Andrieu, V. D. S. Martins, and C.-Z. Xu, "Adding integral action for open-loop exponentially stable semigroups and application to boundary control of PDE systems," *IEEE Trans. Autom. Control*, vol. 65, no. 11, pp. 4481–4492, Nov. 2020.

[54] R. Vazquez and M. Krstic, "Boundary observer for output-feedback stabilization of thermal-fluid convection loop," *IEEE Trans. Control Syst. Technol.*, vol. 18, no. 4, pp. 789–797, Jul. 2010.

[55] J. Wang and M. Krstic, "Output feedback boundary control of a heat PDE sandwiched between two ODEs," *IEEE Trans. Autom. Control*, vol. 64, no. 11, pp. 4653–4660, Nov. 2019.

[56] J. Wang and M. Krstic, "Event-triggered output-feedback backstepping control of sandwich hyperbolic PDE systems," *IEEE Trans. Autom. Control*, vol. 67, no. 1, pp. 220–235, Jan. 2022.

[57] J. Wang and M. Krstic, "Adaptive event-triggered PDE control for load-moving cable systems," *Automatica*, vol. 129, 2021, Art. no. 109637.

[58] J. Wang and M. Krstic, "Regulation-triggered adaptive control of a hyperbolic PDE-ODE model with boundary interconnections," *Int. J. Adaptive Control Signal Process.*, vol. 35, pp. 1513–1543, 2021.

[59] J. Wang and M. Krstic, "Event-triggered adaptive control of coupled hyperbolic PDEs with piecewise-constant inputs and identification," *IEEE Trans. Autom. Control*, to be published, doi: 10.1109/TAC.2022.3159292.

[60] J. Wang, M. Krstic, and I. Karafyllis, "Adaptive regulation-triggered control of hyperbolic PDEs by batch leasts-quares," in *Proc. Amer. Control Conf.*, 2021, pp. 4057–4062.

[61] J. S. Wettlaufer, "Heat flux at the ice-ocean interface," *J. Geophys. Res. Oceans*, vol. 96, pp. 7215–7236, 1991.

[62] Z. Yao and N. H. El-Farra, "Resource-aware model predictive control of spatially distributed processes using event-triggered communication," in *Proc. IEEE 52nd Conf. Decis. Control*, 2013, pp. 3726–3731.

Ji Wang (Member, IEEE) received the Ph.D. degree in mechanical engineering from Chongqing University, Chongqing, China, in 2018.

From 2019 to 2021, he was a Postdoctoral Scholar with the Department of Mechanical and Aerospace Engineering, University of California, San Diego, La Jolla, CA, USA. He is currently an Associate Professor with the Department of Automation, Xiamen University, Xiamen, Fujian, China. His research interests include modeling and control of distributed parameter systems, with applications in cable-driven mechanisms.

Dr. Wang has been an Associate Editor for *Systems & Control Letters* since 2021.

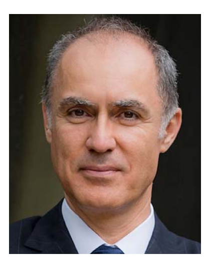

Miroslav Krstic (Fellow, IEEE) received the Ph.D. degree from the Department of Electrical and Computer Engineering, University of California, Santa Barbara, CA, USA, in 1994. He is currently a Distinguished Professor, holds the Alspach Chair, is the founding Director of the Center for Control Systems and Dynamics, University of California, San Diego, La Jolla, CA, USA, and serves as a Senior Associate Vice Chancellor for Research. He has coauthored 16 books on adaptive, nonlinear, and stochastic control, extremum seeking, control of PDE systems including turbulent flows, and control of delay systems.

Prof. Krstic has been an Elected Fellow of IFAC, ASME, SIAM, AAAS, and IET (U.K.), an Associate Fellow of AIAA, and a Foreign Member of the Serbian Academy of Sciences and Arts and of the Academy of Engineering of Serbia. He was the recipient of the Bellman Control Heritage Award, the SIAM Reid Prize, the ASME Oldenburger Medal, the Nyquist Lecture Prize, the Paynter Outstanding Investigator Award, the Ragazzini Education Award, the IFAC Nonlinear Control Systems Award, the Chestnut Textbook Prize, the Control Systems Society Distinguished Member Award, the PECASE, NSF Career, and ONR Young Investigator Awards, the Schuck ('96 and '19) and Axelby Paper Prizes, and the first UCSD Research Award given to an engineer. He is the Editor-in-Chief of *Systems & Control Letters*, has been a Senior Editor of *Automatica* and IEEE TRANSACTIONS ON AUTOMATIC CONTROL, an Editor of two Springer book series, was the Vice President for Technical Activities of the IEEE Control Systems Society, and the Chair of the IEEE CSS Fellow Committee.